TOC-Keyword: Quartz Crystal Microbalance

Advanced Nanoporous Material-Based QCM Devices: A New Horizon of Interfacial Mass Sensing Technology

Nagy L. Torad[+]*, Shuaihua Zhang[+], Wael A. Amer, Mohamad M. Ayad, Minjun Kim, Jeonghun Kim, Bing Ding, Xiaogang Zhang, Tatsuo Kimura* and Yusuke Yamauchi*

Dr. N. L. Torad, Dr. W. A. Amer, Prof. M. M. Ayad

Chemistry Department, Faculty of Science, Tanta University, Tanta 31527, Egypt

E-mail: nagi.kamal@science.tanta.edu.eg

Prof. M. M. Ayad

Institute of Basic and Applied Sciences, Egypt-Japan University of Science and Technology (E-JUST), New Borg El-Arab City, Alexandria 21934, Egypt

Dr. S. Zhang

Department of Chemistry, College of Science, Hebei Agricultural University, Baoding 071001, Hebei, China

This is the author manuscript accepted for publication and has undergone full peer review but has not been through the copyediting, typesetting, pagination and proofreading process, which may lead to differences between this version and the Version of Record. Please cite this article as doi: 10.1002/admi.201900849.

M. Kim, Dr. J. Kim, Prof. Y. Yamauchi

School of Chemical Engineering and Australian Institute for Bioengineering and Nanotechnology (AIBN), The University of Queensland, Brisbane, QLD 4072, Australia

E-mail: y.yamauchi@uq.edu.au

Dr. N. L. Torad, Dr. S. Zhang, Dr. B Ding, Prof. Y. Yamauchi

International Center for Materials Nanoarchitectonics (WPI-MANA), National Institute for Materials Science (NIMS), 1-1 Namiki, Tsukuba, Ibaraki 305-0044, Japan

Dr. T. Kimura

National Institute of Advanced Industrial Science and Technology (AIST), Shimoshidami, Moriyama, Nagoya 463-8560, Japan

E-mail: t-kimura@aist.go.jp

Prof. X. Zhang, Dr. B. Ding, Dr. N. L. Torad

Key Laboratory of Materials and Technologies for Energy Conversion, College of Materials Science & Engineering, Nanjing University of Aeronautics and Astronautics, Nanjing 210016, China

+ These authors equally contributed to this work.

TOC image

Advanced Nanoporous Material-Based QCM Devices: A New Horizon of Interfacial Mass Sensing Technology

By Nagy L. Torad, Shuaihua Zhang, Wael A. Amer, Mohamad M. Ayad, Minjun Kim, Jeonghun Kim, Bing Ding, Xiaogang Zhang, Tatsuo Kimura* and Yusuke Yamauchi**

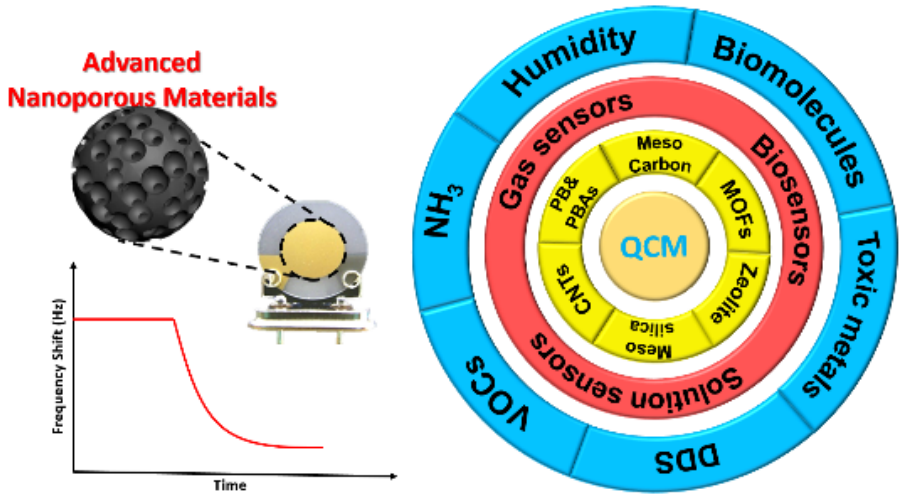

This review introduces an overview of recent advancements in the fabrication of QCM sensing devices for the interfacial mass sensing of targeted chemical vapors and ions through combination with nanoporous materials including mesoporous materials (e.g., silica, metal oxide and metal), carbon-based nanomaterials (e.g., graphene and carbon nanotube), metal-organic frameworks (MOFs), MOF-derived nanoporous carbons, Prussian blue and its analogues (PB and PBA), zeolites and related materials.

Keywords: Mass interfacial processes; Nanoporous materials; Quartz crystal microbalance; Sensing systems; thin films

Authors' photo with short biography

Nagy Torad received his Master degree from Tanta University, Egypt in 2010 under supervision of Prof. Mohamad Ayad. He then moved to Japan for his PhD to study under supervision of Prof. Yusuke Yamauchi at Waseda University, where he graduated in 2014. He worked as a postdoctoral researcher at NIMS and AIST, Japan and NUAA, China. Currently, he is a visiting researcher of NIMS. His research focuses in the synthesis and applications of nanoporous materials for energy and environment-related utilizations.

Yusuke Yamauchi received his Bachelor degree (2003), Master degree (2004), and Ph.D. (2007) from Waseda University, Japan. After receiving his Ph.D., he joined the National Institute of Materials Science (NIMS), Japan to start his own research group. In 2016 he joined the University of Wollongong as a full professor. In Nov 2017, he moved to The University of Queensland (UQ). Currently, he is a senior group leader at AIBN and a professor at School of Chem Eng in UQ.

Tatsuo Kimura studied at Waseda University, Japan and received his Ph.D. degree in 1999. He obtained a permanent research position in National Industrial Research Institute of Nagoya (NIRIN) in 2000 which has been integrated as the AIST Chubu of National Institute of Advanced Industrial Science and Technology (AIST) since 2001. He has researched a wide variety of surfactant assisted mesoporous materials (e.g., oxides, phosphates, and inorganic-organic hybrids) and mainly focused on the precise structural design in the molecular scale including the morphological variation for utilizing as advanced materials of adsorbents, catalysts, electrodes, etc.

Abstract

Mass interfacial processes have been considered as one of crucial factors supporting fundamental researches. Importance of such interfacial processes has encouraged development of methodologies that can sense mass changes at the surfaces of deposited powders and thin films. Due to the low cost and conceptual simplicity of these processes, significant advancements have been achieved by piezoelectric methods for in situ determination of minute mass changes on the surfaces of materials under various conditions. These methods portend the extensive development of researches and commercial applications related to sensor technology, electroplating, and corrosion. Introduction of nanomaterials for designing sensors and monitoring systems becomes essential to create advanced detection systems for sensing of toxic materials for environmental remediation. Integration of materials with predesignated nanostructures into sensor devices, such as surface acoustic wave (SAW), quartz crystal

microbalance (QCM) and quartz crystal microbalance with dissipation (QCM-D) monitoring has led to an immense progress in the sensing applications of toxic target analytes at the nano-gram range. Of the various classes of mechanical sensors, this review introduces an overview of recent advancement in the fabrication of piezoelectric devices, such as QCM and QCM-D sensing devices for the interfacial mass sensing of targeted chemical vapors and ions through combination with nanoporous materials including mesoporous materials (e.g., silica, metal oxide and metal), carbon-based nanomaterials (e.g., graphene and carbon nanotube), metal-organic frameworks (MOFs), MOF-derived nanoporous carbons, Prussian blue and its analogues (PB and PBA), zeolites and related materials. Challenges and future prospect are also summarized by the advanced QCM technique associated with properties of nanostructured materials.

1. Introduction

1.1. Piezoelectric effect

In 1880, Jacques and Pierre Curie discovered that the magnitude of resulting electrical potentials across various crystals such as quartz, tourmaline, and Rochelle salt ($NaKC_4H_4O_6{\cdot}4H_2O$) was proportional to the stresses that are mechanically induced at the surface of the crystals,[1] being called the "piezoelectric effect" (derived from the Greek word *piezein,* which means "press"). In particular, generated charge across the quartz crystal through the mechanical stress resulted from the dipole formation that was generated by the displacement of atoms in an acentric crystalline material. Shortly after the discovery, the Curies proved experimentally the so called "converse piezoelectric effect" when they found the relationship between voltage across these crystals and

mechanical strain (motor generator). Combined with the piezoelectric effect, the later insight was eventually utilized for the development of electromechanical devices and underwater sound transducers (sonar), including phonograph pickups microphones and speakers.[2]

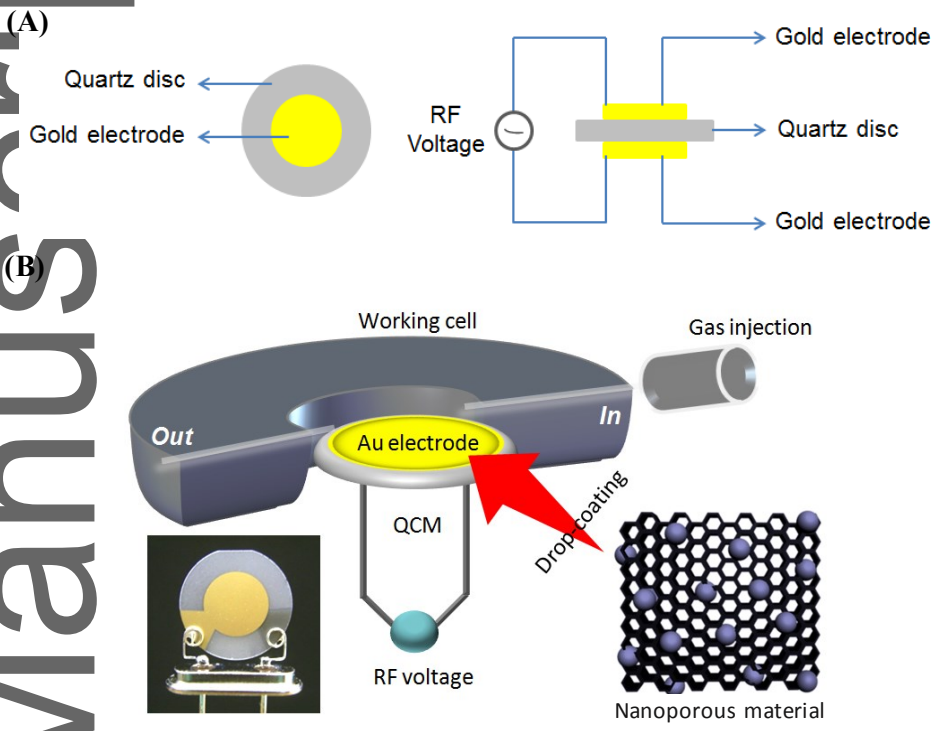

Figure 1. Schematic representation of (A) QCM and (B) the interaction between the target molecules and an active layer coating on QCM electrode.

The very stable oscillator circuits are constructed depending on the converse piezoelectric effect, thereby applying an alternating electric field in the quartz crystal that results in a corresponding alternating strain field. A corresponding vibrational or oscillatory motion is generated in the quartz crystal as a result of the strain field, causing the formation of acoustic waves. Of particular interest, the quartz oscillator strongly prefers to vibrate at a characteristic resonance frequency, and impedance analyses generally reveal sharp conductance peaks at this frequency, indicating a

high-quality factor (*Q*), which is the ratio between energy stored and energy dissipated per cycle (*Q* values can exceed 100,000). Because of the minimal energy dissipation of quartz crystals, in addition to their low cost, low defect concentration, ruggedness, chemical inertness, and ready fabrication, they are nearly ideal oscillators and then widely utilized in frequency control and filter circuits.[2] The piezoelectric effect occurs normally in crystals without a center of symmetry. Clearly, the applied pressure across the crystal induces a deformation in the crystal lattice in such a way that a corresponding dipole moment arises in the molecules of the crystal.[3] After slicing a single crystal quartz wafer, quartz discs are sandwiched as the piezoelectric quartz crystal (PQC) between a pair of electrodes which are generally composed of gold or silver deposited by thermal evaporation process (**Figure 1A**). The PQC device can detect the difference in an alternating electric field between the electrodes. In this regard, a physical orientation of the quartz crystal lattice is distorted due to an applied voltage, resulting in the mechanical oscillation by a standing shear wave across the quartz crystal disc at a characteristic vibrational frequency (i.e., the natural resonant frequency of the quartz crystal).[3] Direction of the oscillation strongly depends on the crystal lattice orientation in an electric field. Thus, oscillation in the thickness shear mode (TSM) creates a displacement parallel to the quartz disc surfaces and the area of the quartz disc located between metal electrodes is only piezoelectrically active. The maximum amplitude of oscillation is then achieved when the electrode pads overlap and diminishes rapidly from that point.[3]

1.2. Quartz crystal microbalance

In the Quartz crystal microbalance (QCM), parameters associated with phases adjacent to the crystal greatly affect the frequency change of the quartz crystal, along with the physical properties of the crystal itself, such as size, cut, density and shear modulus.[4] For analytical sensing devices, the

proportional relation between the QCM crystal resonant frequency and its overall mass is of particular importance because this relationship is frequently utilized in most of piezoelectric analytical applications.[5] A decrease in the QCM resonant frequency is obtained due to a deposition of mass over its surface and the mass sensitivity of QCM is largely dependent on the crystal thickness, which determines its resonant frequency. As illustrated in **Figure 1A**, QCM consists of a quartz disk coated with metal electrodes on both sides. When a voltage is applied to the quartz crystal plate, it can oscillate at a specific frequency and the relation between frequency change (ΔF) of the oscillating crystal and the mass change (Δm) on the quartz surface was described by Sauerbrey empirical derivation (Eq. 1).[6] The dynamic change of ΔF (Hz) in the area of the electrode (A / cm^{-2}) in terms of the mass increment, Δm (g cm^{-2}) loaded onto the crystal surface under a certain resonant frequency F_0 is shown in Eq. 1, where N, F_0, ρ, μ, and A are the harmonic overtone, the fundamental resonance frequency, the crystal density (2.649 g cm^{-3}), the elastic modulus of the quartz crystal (2.947×10^{11} g cm^{-1} s^{-2}), and the surface area (5 mmΦ, 0.196 cm^2), respectively.

$$\Delta F = \frac{2NF_0^2}{\sqrt{\rho\mu}}\frac{\Delta m}{A} \qquad (1)$$

QCM sensor technology has been widely utilized for measuring small changes of mass deposited on its electrodes in nano-gram (ng) range. During the past few decades, the relationship between frequency shift and mass change, which was initially described by Sauerbrey, has been extensively applied for chemical sensing.[7-8] The frequency shift, which is proportional to a mass adsorbed and/or sorbed on sensitive layers coated over the QCM electrode, is constantly monitored to identify and quantify the target analyte. Accordingly, the interaction between target molecules and sensitive coating layers (known as “guest-host interaction”) plays an important role in the sensing mechanism. Such a guest-host interaction is considered as an adsorption process involving enrichment of guest species at the interface of a certain adsorbent (**Figure 1B**). Since 1964, A QCM

device had been implemented by King into a gas chromatography system for the detection of hydrocarbons.[9] So far, QCM sensor device has been successfully applied as a sensitive tool to sense mass interfacial,[10] thin film viscoelasticity,[11-12] polymer film properties,[13-16] bulk liquid viscosity and density.[17-18] In addition, combination of the QCM technique with electrochemical methods was realized for in situ measurements of mass changes which took place during adsorption, underpotential deposition, and dissolution of surface films.[19-20] Accordingly, ΔF was investigated in terms of rigid mass changes, based on the Sauerbrey equation. However, in liquids, the response of QCM electrode is influenced by various factors such as morphology of surface films, interfacial liquid properties, and on the solid/liquid coupling at the interface, thus ΔF is not well-consistent with that estimated by Saurbrey equations (Eq. 1).[21-23]

The Sauerbrey equation is usually disturbed by the changes in liquid properties and the longitudinal wave effect when QCM is operated in the liquid phase.[24-28] The first attempt to use an acoustic device as a liquid phase sensor was reported by Konash and Bastiaans in 1980.[29] Two years later, the pioneering studies to define the parameters govern the change in the QCM frequency in liquid phase systems have been reported by Nomura and Okuhara.[30] Further investigations demonstrated the validity of the Sauerbrey's equation, especially if the solutions are not highly viscous and only one electrode is contacted with solution, being in a good experimental agreement with the prediction by Buckenstein et al.[17] and Kanazawa et al.[31] From a hydrodynamic view point, liquids differ from each other by their specific density (ρ) and dynamic viscosity (η). Kanazawa and Gordon proposed the relationship between mass and frequency change taking account into the viscoelastic effects on the electrode surface (Eqs. 2 and 3),[32] where, ΔF is the frequency change before and after reaction (Hz), ΔR is the resonant resistance change (Ω), ρ_q is the quartz density (2.65 g cm^{-3}), μ_q is the quartz shear stress (2.95×10^{11} g cm^{-1} sec^{-2}), n is the overtone order, ρ_L is the binder density (g cm^{-3}), η_L is the binder viscosity (cP), and ω_s is the nominal frequency (Hz).

$$\Delta F = -F_u^{3/2} \sqrt{\frac{\rho_L \eta_L}{\pi \mu_q \rho_q}} \quad (2)$$

$$\Delta R = (n\omega_s L_1/\pi) \sqrt{\frac{2\omega_s \rho_L \eta_L}{\mu_q \rho_q}} \quad (3)$$

Changing in viscosity of liquid always occurs changes in frequency and signal attenuation of the liquid-phase QCM sensor, use of an appropriate algorithm is necessary to separate out the effects. To overcome this experimental concern, Kang et al. reported another an associated high-frequency resonance (HFR; the total resonance originating from the network including leading wire inductance, static QCM capacitance, solution capacitance, and solution inductance) model for QCM, with an intensity two orders of magnitude higher than that of the fundamental peak in the liquid phase.[33] The HFR intensity did not dampen in nonelectrolyte liquid despite of its viscosity. By excluding the additional frequency shifts resulting from the shift of the HFR peak and the changes in viscosity and density of the liquid phase, the frequency response of QCM is neglectful. The stability of QCM in TSM was totally improved after correcting the influences comes from HFR. Some abnormalities in the frequency response of QCM in high order overtone was still understandable in a case using the HFR resonant model. However, this finding will be helpful for obtaining more reliable information from the QCM responses important for exploring potential applications such as chemical and biological sensors. A designed QCM setup was reported for the use in viscous liquids at high temperatures above 300 °C.[34] The QCM crystal deposited with iron and gold responded to two common lubricant base oils, polyalphaolefin and halocarbon, being consistent with theoretical predictions that incorporate electrode nanoscale surface roughness into their analysis.

The influence of surface roughness on a QCM response in contact with liquids having a wide range of viscosity and density was also studied, based on the perturbation theory to describe effects of the

slight roughness and Brinkman's equation for strongly rough surfaces (pores, cavities and bumps).[35-37] Consequently, it was found that ΔF was proportional not only to the effect of the inertial motion of a liquid mass rigidly coupled to the surface but also to the additional viscous energy dissipation in the interfacial layer induced by roughness. And then, a relation between QCM response and interface geometry was utilized for analyzing effects of roughness and rough electrode surfaces. An adsorbed layer surface roughness on the QCM-D response was also investigated with an emphasis on determining the amount of trapped water.[38] Very recently, QCM-D was used for a real-time gravimetric and hydrodynamic spectroscopic characterization of porous solid deposits (interfaces) formed dynamically on the QCM electrode in contact with a liquid.[39] A hydrodynamic correction to the Sauerbrey equation was derived depending crucially on the porous structure parameters of the solid. In both cases of the intrinsically porous solid layer on the crystal surface with a flat external surface, called a homogeneous porous layer (slight roughness) and the complicated one which contains micron-sized spherical bumps or aggregates (known as non-homogeneous solid porous layers, strong roughness), the related total frequency and resonance width changes for the response in liquid are expressed by the hydrodynamic admittance models for the in situ sensing of rough/porous solid layers.[39] When the fundamental frequency (F_0) is being used, variations in penetration depth (δ) are possible by using liquids with different viscosity-to-density ratios. Therefore, by varying the penetration depth, the entire variety of lateral pore sizes in the porous solid can be easily screened to distinguish between the trapped and moveable liquid in the narrow and wide pores, respectively. However, for electrolytically-deposited porous solid layers using EQCM-D, the hydrodynamic correction to the mass effect can be roughly estimated by the combination of the Faraday law and the Sauerbrey's equation, whereas the mass of the deposited porous solid layer is translated into the related frequency change).[39]

The design and application of coating QCM electrodes for discriminating and/or responding to particular targets is very crucial because the useful sensing tool requires high sensitivity and

selectivity. In the sense of applications, the fabrication of nanoarchitectonics materials is an important step towards the development of efficient advanced detection sensors. Change in the QCM frequency corresponds to the mass of adsorbed analyte in ng cm^{-2}. For instance, the conventional AT-cut 9 MHz QCM sensor can ideally sense a mass change with a higher sensing capability at the ng-level of much lower concentration of target guests after careful modification of the electrode surface with advanced nanoporous materials. Such materials with regular pore geometries, such as mesoporous materials, MOFs, and patterned films, have received much attention as effective media for sensing, sorption, and storage of materials due to their structural features like high surface area and pore volume per unit mass. From the viewpoint, researches on adsorption of guest molecules into nanospaces have become one of the important issues of nanoscience. Herein, we review the focus on adsorption inside advanced nanospaces by applying the QCM sensing device for various chemical and biological sensing applications.

2. Advanced nanoporous material-based QCM sensors

Adsorption and/or diffusion of some inorganic and organic gases and chemical vapors, such as nitrogen (N_2), toluene ($C_6H_5CH_3$) and water (H_2O), were studied by utilizing the QCM sensing device through modification onto its metal electrode with a variety of porous materials.[40] Materials nanoarchitectonics for bioanalytical sensing applications, such as mesoporous materials, 2D materials, fullerene, and supported lipid bilayers coated QCM and QCM-D sensor were also employed for the detection of toxic gases, cell membrane interactions, anticancer drug evaluation, label-free biomolecular assays, complement activation-related multiprotein membrane attack complexes, and label-free biomolecular assays, which are partially supported by data analysis, such as principal component analysis.[41,42] The QCM technique can also be employed for evaluating

adsorption properties of some porous materials in the liquid and gas phase. Even when powder materials are directly deposited over the electrode, adsorption properties due to their porous structures are also investigated by using the same device. To improve sensitivity, reproducibility, and response/recovery speed of the QCM sensor device, the use of nanoporous molecular sieves and well-designed nanostructured sensing materials having high surface area and large pore volume is quite interesting. After the modification of the electrode with such nanoporous materials, sensing properties mainly depend on the physical and the chemical properties of the nanoporous materials. From the viewpoint, diverse nanoporous materials including mesoporous silica-based materials, carbon-based nanomaterials, hybrid inorganics, porous coordination polymers (PCPs), and zeolites are highlighted for the QCM-based sensing utilizations.

2.1. Mesoporous materials

2.1.1. Silica-based mesoporous materials

Numerous attentions have been paid to the detection of hazardous chemical agents such as formaldehyde that causes probable human carcinogen, allergen, and intense irritant for eyes and mucous membranes. One of the most challenging and vital issues is, thus, setting selective techniques for the accurate evaluation of environmentally hazardous chemicals including volatile organic compounds (VOCs) and toxic metal ions.[43] Especially, researchers are interested in the fabrication of highly efficient sensors for enhancing the environmental and safety control of pollutants. For a high adsorption capacity, selection of adsorbents, which are composed of well-ordered and fully interconnected pores with excellent textural parameters, are crucial to get high adsorption capacity.[44] Mesoporous silica is considered as one of the most promising hosts for wide application fields in nanoscience, especially those fields that are related with the ability to

affect the guest dynamics in the host matrix.[45] Here, we categorize the sensing properties of QCM-based mesoporous silica materials for in situ detection of environmentally hazardous pollutants.

Volatile organic compounds. Silica-based mesoporous hybrids attaching organic functions are regarded as ideal candidates in the chemical sensing field. Continuous porous networks also help to realize smooth molecular diffusion and hence an enhanced sensitivity[46] The good chemical and thermal stability[47] enable stable sensing properties. Abundant silanol (Si-OH) groups over the silicate frameworks make them great hosts for incorporating various organic groups. Therefore, tailor-made active materials can be designed to achieve specific molecular detection. For example, it was reported that amine-functionalized SBA-15 type mesoporous silica was successfully designed by using a post-grafting method.[48] The SBA-15 type composite with unique short vertical channels led to a uniform functionalization of amine (-NH_2) groups Several researchers have also studied the sensing properties of NH_2-SBA-15 coated QCM sensors toward hazardous vapors.[49] The advantages of this sensor arose from its low cost, the large adsorption capabilities, the fast adsorption rate, and the good chemo-selectivity to formaldehyde molecules with a ppb-level detection limit, as compared to conventional SBA-15 type pure silica, due to a specific interaction between analytes and organic functional groups.

The sol-gel process combined with an argon plasma calcination technique was employed for the fabrication of mesoporous silica films that were subsequently deposited on the flat gold electrode surface of the QCM sensor.[50] The technique of plasma calcination involves the turning of silica sol into its gel at low temperature instead of the conventional process of thermal calcination. The resultant films were used for gas sensing applications by entrapping sensitive materials in the porous network. Employing the anti-Markovnikov reaction, β-cyclodextrin (β-CD) was included in the silica

film via alkenylation of the hydroxyl groups and thiolation of the film itself for enhancing the detection of benzene (C_6H_6) and ethanol (C_2H_5OH) vapors. The β-CD/silica hybrid film-coated QCM sensor was subjected to 5-500 μL of C_6H_6 and C_2H_5OH into 8 L sealed gas chamber and exhibited its higher frequency response. The enhanced QCM response arose from the large surface area of the mesoporous silica films that results in accommodating more receptor (β-CD) molecules and more target analytes as well.[51] Five months later, the same authors[52] extended the use of for the fabrication A four-channel QCM array (QCA) was fabricated by the standard photo-lithography in combination with the plasma calcination technique. The QCA sensor was examined for the detection of C_6H_6 and alcohol vapors. Employing the covalent linkages and/or physisorption, sensitive materials such as β-CD and triphenylphosphine were introduced into the mesopores surrounding silica frameworks and then utilized for distinguishing between alcohol and C_6H_6 vapors in the ppm range.

A soluble guanylyl cyclase (sGC), as a nitric oxide (NO) specific hemoprotein, was entrapped into a network of mesoporous silica. A 10 MHz AT-cut QCM coated with the network was applied for the detection of NO in the gaseous state.[53] Polyethylene glycol with a low molecular weight served as an organic template for a sol-gel derivative porous silica film. The strong affinity of NO molecules with the ferrous heme(s) of sGC enabled a high detection sensitivity of about 15 ppb/Hz. The frequency response of the QCM sensor was not influenced by the chamber temperature or the pressure. Minimal interferences were found with other species such as carbon monoxide (CO) and nitrogen dioxide (NO_2) and therefore utilized for the selective detection of NO molecules. When the QCM electrode was covered with a mesoporous silica film functionalized with covalently attached propyl groups , the water content in the propyl-functionalized mesoporous silica film was analyzed at different relative humidity.[54] A fully reproducible and reversible water absorption process was observed for the composite film showing an increase the relative humidity from 30% to 80%, while

the existence of a much larger amount of water was confirmed by using the corresponding pure silica film.

Toxic metal ions. Pollution containing heavy metals, especially Hg^{2+}, is a serious environmental problem[55-57] and the detection of its traces in wastewater is thus of substantial demand.[58-59] Compared with conventional detection methods,[60-62] such as colorimetric assay, cold-vapor atomic absorption spectrometry (AAS), and inductively coupled plasma spectroscopy (ICP), etc., QCM-based sensors are more desirable because they are portable enough for on-site monitoring of heavy metal ions in the real environment. Inspired by the functionalization of SBA-15 type mesoporous silica with terminal thiol group (-SH) for chelation with Hg^{2+} in water,[63-64] such a SH-functionalized SBA-15 (SH-SBA-15) was coated over QCM transducers for designing an Hg^{2+} sensor.[65] Specific surface area and pore size were the key factors for the Hg^{2+} detecting capability in water. The selectivity of SH-SBA-15 coated QCM sensors toward Hg^{2+} was very high even in the presence of other cations, such as Na^{+}, K^{+}, Mg^{2+}, Fe^{3+}, Cu^{2+}, Zn^{2+}, and Cd^{2+} ions.

Humidity and water vapor. The on-line monitoring and in situ detection of humidity and water vapor is very important in the research field of sensors. By using polystyrene-*block*-polybutadiene-*block*-polystyrene (PS-PB-PS) triblock copolymers, which contained hydrophilic sulfonic ($-SO_3H$) groups attached to the polystyrene (PS) block, mesoporous silica films was successfully fabricated with the formation of spherical mesopores.[66] Thickness of the silicate frameworks related to the pore-to-pore distance mainly depended on the amount of the copolymer without a significant change of the pristine diameter of the spherical mesopores. A hierarchical porous system showing the high sensing capability of water was very helpful for designing a unique QCM sensor for the on-line monitoring even in the humidity level. Upon exposure of the designed

QCM sensor to water vapor, the frequency of the quartz crystal electrode was decreased with the adsorption of water molecules. A very fast diffusion of water molecules was observed in an early stage of the sensing using the highly porous silica coated electrode. Adsorption kinetics of water molecules was investigated further by real-time pursuing the frequency change after introducing water vapor into the QCM chamber and determining the diffusion coefficient (*D*) by applying the Fickian model as a simple linear adsorption model.[67] The uptake process was found to obey the Fickian diffusion model with a very fast uptake rate and thus shortening the diffusion pathway length and increasing the diffusion coefficient. The experimental data was analyzed using Fick's second equation;[68] the relation of $\Delta F_t/\Delta F_\infty$ vs. $t^{1/2}/L$ was plotted and the *D* value was obtained from the first linear portion of the diffusion line according to the following equation 4, where, ΔF_t refers to the frequency change at time *t*, while ΔF_∞ refers to the frequency change at the end of the diffusion process.

$$\frac{\Delta F_t}{\Delta F_\infty} = 4\sqrt{\frac{D}{\pi}}\frac{t^{1/2}}{L} \qquad (4)$$

Both of ΔF_t and ΔF_∞ can be respectively given as the following equations 5 and 6, where, F_t refers to the frequency at time *t*, F_∞ expresses the equilibrium state frequency, and *f* refers to the parent frequency of the oscillator.

$$\Delta F_t = F - F_t \qquad (5)$$

$$\Delta F_\infty = F - F_\infty \qquad (6)$$

The adsorption kinetics of water vapor were investigated by applying pseudo-first-order mass transfer between the vapor phase and mesoporous silica layers assuming that the surface concentration of water vapor is constant and the diffusion through the mesoporous silica layers is

governed by the concentration gradient through the sample. Therefore, the rates vapor uptake can then be compared by determining the pseudo-first-order rate constant (k) in the following equation 7,[69] where, ΔF_t and ΔF_∞ are the frequencies of vapor uptake at time t and at equilibrium, respectively. Moreover, the initial water vapor uptake by the mesoporous silica was confirmed to be very fast and the existence of large difference in the diffusion uptake at the initial stage can be interpreted by the retention of water molecular inside the small mesospace.[66]

$$\frac{\Delta F_t}{\Delta F_\infty} = 1 - e^{-kt} \qquad (7)$$

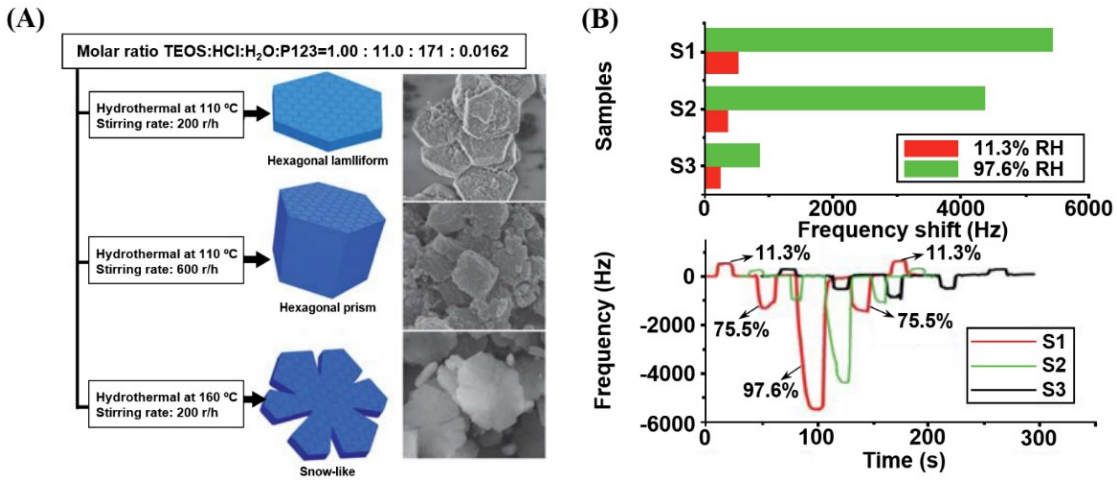

Figure 2. (A) Schematic description of the formation of SBA-15 with different morphologies. (B) frequency response curves of S1, S2, S3 in low (RH = 11.3%) and high (RH = 97.6%) relative humidity and typical time-dependence of the S1, S2, S3 measured by the humidity cycle. Adapted with permission.[70] Copyright 2011, The Royal Society of Chemistry.

A facile synthetic strategy of monodispersed SBA-15 type silica was developed with the macroscale design to hexagonal prism, hexagonal lamelliform, and snow-like morphologies (**Figure 2A**) via a hydrothermal route in an acidic medium by changing the stirring rate in a hydrolysis process of tetraethylorthsilicate (TEOS) using a triblock copolymer, Pluronic P123, poly(ethylene oxide)-*block*-poly(propylene oxide)-*block*-poly(ethylene oxide) ($EO_{20}PO_{70}EO_{20}$).[70] However, self-assembled hexagonal plate-like uniform particles were obtained hydrothermally in an acidic medium employing another triblock copolymer, Pluronic F127, as the structure directing agent with an addition of KCl and 1,2,4-trivinylcyclohexane.[71] When such SBA-15 type silicas were deposited on the QCM electrode, highly stable and sensitive humidity sensors were successfully fabricated with a wide response of the relative humidity (RH) ranging of 1-100% (**Figure 2B**). Usage of three QCM sensors coated with the same thickness of hexagonal lamelliform (S1), hexagonal prisms (S2), and snow-likes (S3) SBA-15 type silicas gave us the response to low (11.3%) and high (97.6%) RH (**Figure 2C**). Upon increasing the BET surface area (the hexagonal lamelliform SBA-15; 733 $m^2\ g^{-1}$), the frequency was shifted under the same humidity conditions and the highest sensitivity, 66.4 Hz/%RH was obtained as well. Due to the large surface area with the availability of multiple Si-OH groups over the pore surfaces, the large amount of water molecules can be adsorbed over the surfaces of SBA-15 and then large mass changes are observed, being related to the high sensitivity to humidity. Thus, the hexagonal lamelliform SBA-15 (S1) having the highest BET surface area and short vertical channels exhibited better humidity response than those observed for other SBA-15 type silicas (S2 and S3) with lower BET surface areas and short vertical channels.[70]

By using surfactant-containing mesoporous films of silica modified with short alkyl chains, a diffusion behavior of terrylene diimide dye molecules inside the mesoporous network was visualized by utilizing single-molecule fluorescence microscopy.[54] During this innovative research, diffusion of the dye molecules was investigated by using methyl-, ethyl-, and propyl-functionalized (10 mol%

density) films at different RH (30%, 50%, and 80%). The mean diffusion coefficient was increased from 1100 to 3870 $nm^2 s^{-1}$ by increasing the humidity from 30% to 80%. Upon increasing the water content from 30% to 80 % RH, the mean diffusion coefficient of the dye molecules was also increased under the comparable conditions by a factor of 2.8. From the QCM measurements, the amount of water absorbed in the as-synthesized composite films was confirmed from 30% to 80% RH in a fully reversible and reproducible manner.

Drug delivery systems. A QCM technique was applied for investigating the loading capability of ketoprofen (KP) and 5-flurouracil (5-FU) drugs over an amine-functionalized KIT-6 type mesoporous silica (NH_2-KIT-6). Among several advantages of NH_2-KIT-6, high mechanical and chemical stability in addition to high surface area were attractive and then provided the opportunity for designing excellent drug delivery system (DDS). Thin layer of sodium polystyrene sulfonate/polydiallyl dimethyl ammonium chloride was assembled over the QCM electrode after drop-coating (deposition) of NH_2-KIT-6 (36.0 μg cm^{-2}) and then the amine-functionalized electrode was exposed to KP and 5-FU in a buffer solution eat around pH 4. Frequency of the electrode was decreased with the increase of the magnitude of ΔF, which revealed the successful loading of KP and 5-FU drugs. The maximum percentages of their loadings were 1.00 mg g^{-1} and 0.88 mg g^{-1}, respectively. The loading of KP higher than that of 5-FU was attributed to the acidity of KP due to the presence of carboxylic and carbonyl groups that can be interacted with the surface NH_2 groups of NH_2-KIT-6.

In the similar way, KIT-6 and SBA-15 were functionalized with sulfonated group (SO_3H-KIT-6 and -SBA-15) and used for investigating the loading of procaine hydrochloride (PrHCl) drug.[72] As a local anesthetic drug, PrHCl was loaded in ordered mesoporous silica to design a controlled DDS system that can be employed for relieving the pain of the general intramuscular injection in general of

penicillin and the dental anesthesia in particular. The SO_3H-KIT-6 and -SBA-15 modified (32.0 μg cm^{-2}) QCM electrodes were treated with a PrHCl solution, showing the loading efficiency of 1.28 mg g^{-1} and 0.87 mg g^{-1}, respectively. The high loading of PrHCl molecules onto SO_3H-KIT-6 was arising from the large pore diameter induced by its 3D cubic mesostructure related to a fast diffusion of PrHCl molecules combined with the high surface area. In addition, the PrHCl uptake greatly increased by grafting -NH_2 and -SO_3H groups through covalent bonds to surface Si-OH groups.

Enzymes immobilization. Immobilization of enzymes into mesopores are very interesting for exploring potential applications to biocatalysis and biosensing. However, actual understanding of the immobilization process has not been completed so adequately. In this context, QCM with dissipation monitoring (QCM-D) was a facile and robust measuring technique for real-time studying the immobilization of enzymes.[73-75] A novel QCM-D method was demonstrated for understanding the immobilization of enzymes into mesoporous silica particles,[73] which complemented other conventional enzyme monitoring entrapment approaches that were able to detect the concentration depletion only in the surrounding bulk phase. In this regard, silica coated electrode was modified with -HN_2 groups, followed by adsorption of small particles of spherical mesoporous silica. For two different enzymes, lipase from Rhizopus oryzae and feruloyl esterase from Fusarium oxysporum, adsorption behavior was monitored in real-time by using QCM-D monitoring. The QCM-D measurements showed the porosity of mesoporous silica particles was useful for the immobilization of the enzymes. A viscoelastic effect of the immobilized enzymes was also visualized by plotting the frequency shift of the QCM frequency versus the corresponding dissipation. A lysozyme specific aptamer can also be fixed onto an amine-functionalized MCM-41 (NH_2-MCM-41)

particles by a glutaraldehyde coupling, which was applied for the QCM-based determination of lysozyme from chicken egg white.[75]

2.1.2. Non-silica-based mesoporous materials

The detection of chemical vapors was enhanced by the coating of Au electrode with high-surface area mesoporous materials for gravimetric QCM sensing, referred to as the "meso-QCM system" and this was previously reported by our group (**Figure 3A**).[76] Coating of the QCM electrode with high-surface-area mesoporous materials led to the successful evaluation of C_2H_5OH and CH_3CHO vapors with the detection limit less than 1 ppm. The quantitative analysis of mixed chemical vapors was also demonstrated by using the sensing properties arising from the difference between silica and aluminophosphate (AlPO). Therefore, one of the challenges is the pioneering design of the framework composition in addition to the structural features such as the mesoporous structure (mesopore size, dimension/connectivity, etc.) so as to improve the sensitivity and the selectivity of sorption properties beside looking for new and/or advantageous functions that improve the sensing of the meso-QCM system. Due to the selective interaction of the framework surfaces with VOCs like CH_3CHO, the AlPO-based meso-QCM system can be considered as an encouraging sensor for the quantitative determination in the ppb range. As illustrated in **Figure 3B**, a wide variety of VOCs are quite sensitive to the surface properties of mesoporous materials including carbon-based amorphous and graphitic ones.[77] In the case using electrodes coated with carbon-based materials, C_6H_6 molecules hardly adsorbed over amorphous carbon frameworks and more attached with graphitized surfaces due to their strong π-π interaction. $C_6H_5CH_3$ molecules were also captured over the graphitized frameworks, though little *c*-C_6H_{12} without π electrons was detected even by using the graphitized mesoporous carbon. On the other hand, a soluble and shape-persistent organic cage

compounds was deposited by using an electrospray method, showing the extraordinary affinities to the vapors of aromatic solvents.[78]

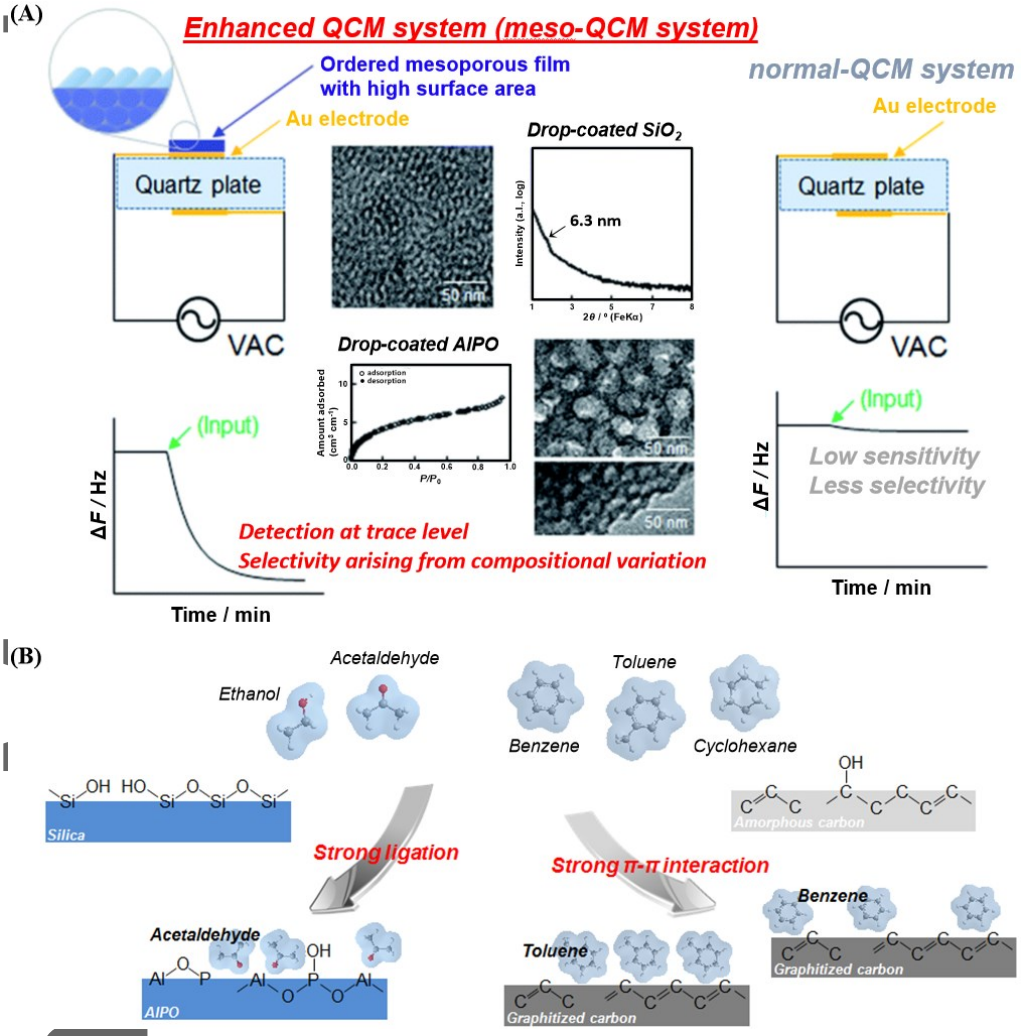

Figure 3. (A) Meso-QCM sensing system enhanced by coating the parent Au electrode with Pluronic P123 assisted mesoporous silica and AlPO materials, compared with an unmodified QCM system. (B) Selective interactions of chemical vapors for the trace-level detection by the meso-QCM systems combined with surfactant-assisted mesoporous silica- and AlPO-based materials as well as carbon-based mesoporous materials. Adapted with permission.[76] Copyright 2014, The Royal Society of Chemistry.

Several metal nanostructures, such as CdSe, SnO_2, TiO_2, ZnO, WO_3, and ZnS, are good candidates for the fabrication of semiconductor-based sensors.[79-83] Sensing performance of such materials is mainly controlled by their properties including morphology, porosity and conductivity. Some active metals, such as Au, Pd and Pt, are also included into these semiconductors-based sensors.[84-89] Catalytic performance for different applications, such as catalytic reduction of carbon dioxide (CO_2),[90] sensing of different VOCs,[91] production of hydrogen (H_2),[92] and oxidation of H_2 to water (H_2O),[93] was enhanced by the strong interaction between Pt and TiO_2 that was also useful in reactions in fuel cells.[94] In the regard of the considerable surface area and available large pore volumes, mesoporous/nanoporous TiO_2 are promising for capture of the metal nanoparticles.[95,96] After in situ liquid-phase analytical method was developed for studying the adsorption kinetics of dyes to a mesoporous TiO_2 coated QCM sensor,[95] a polymeric micelles assembly technique was applied for construction of Pt-decorated mesoporous TiO_2 showing the sensitivity toward several organic molecules (**Figure 4A**).[96] The crystalline mesoporous TiO_2 decorated with uniformly dispersed Pt nanoparticles was synthesized by the polymeric micelle self-assembly of an asymmetric poly(styrene-*b*-2-vinylpyridine-*b*-styrene), PS-*b*-PVP-*b*-PEO, triblock copolymer in an acidic solution of tetrahydrofuran (THF), being challenging in a nanoparticle synthesis as shown in **Figure 4A**. This method was quite facile because it enabled a one-pot synthesis of the crystalline mesoporous TiO_2 with Pt nanoparticles through strong hydrophobic interaction of Pt(II) 2,4-pentanedionate with the PS core and electrostatic interaction of titanium tetraisopropoxide with the PVP shell. The superior affinity of the designed QCM sensor coated with Pt-decorated mesoporous TiO_2 was very promising for highly selective detection of acetaldehyde vapors, which was 7 times greater than that in case of ethanol.

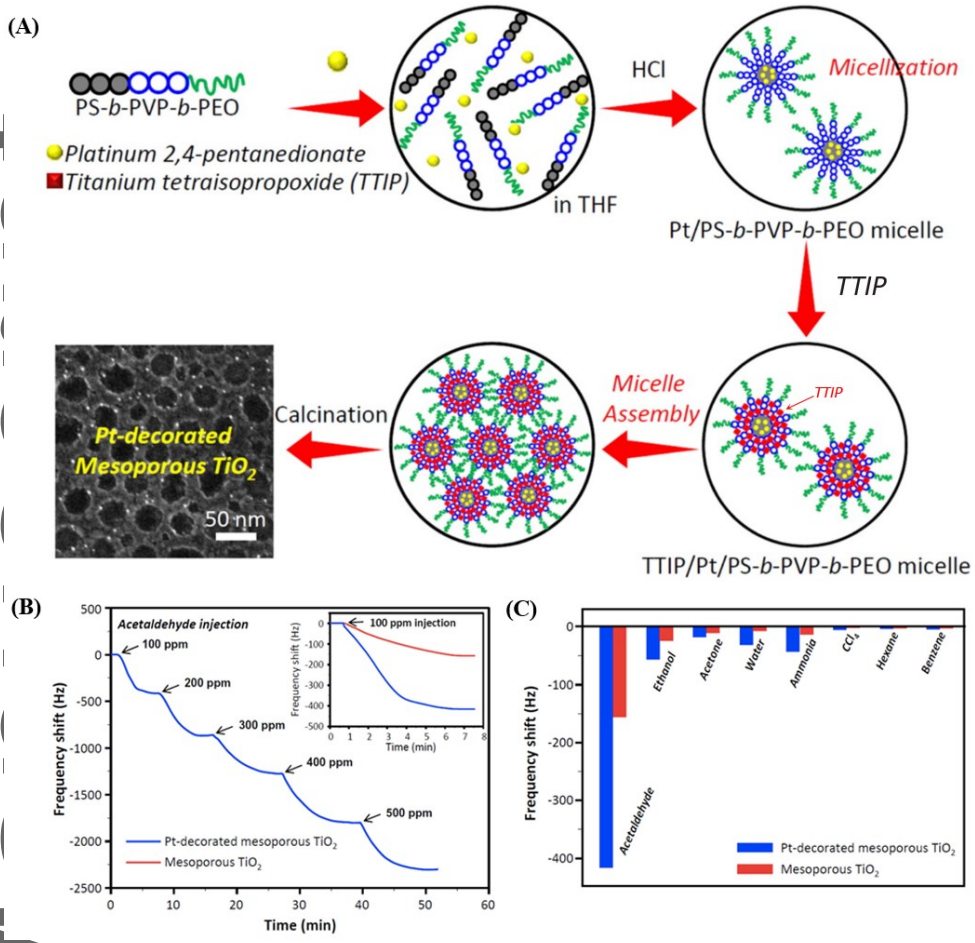

Figure 4. (A) Schematic illustration of the synthetic process of Pt-decorated mesoporous TiO_2 by polymeric micelle assembly. (B) Typical mass-normalized time-dependent frequency shift (ΔF) curve of QCM coated with pure mesoporous TiO_2 (red line) and Pt-decorated mesoporous TiO_2-based films (blue line) caused by exposure to different injected concentrations of vaporized acetaldehyde. (C) Summary of QCM frequency shifts of mesoporous TiO_2-based films (red line) and Pt-decorated mesoporous TiO_2-based films (blue line) caused by exposure to various vaporized gases at 100 ppm. Adapted with permission.[96] Copyright 2014, American Chemical Society.

Adsorption of CH_3CHO, considered as a possible carcinogenic agent to humans by the International Agency for Research on Cancer of the World Health Organization (WHO|IARC) as it is classified as a highly reactive and odorous organic compound,[97] was remarkably risen upon increasing its injected concentration that coincides with the sensing behavior of *n*-type semiconductor sensors.[98] The frequency shift of the Pt-decorated mesoporous TiO_2-based QCM sensors was increased exponentially and linearly with the concentration of injected CH_3CHO from 100 to 500 ppm (**Figure 4B and 4C**). The QCM sensor exhibited a 2.5 times higher response to CH_3CHO vapors than the QCM sensor based on a corresponding (Pt-free) mesoporous TiO_2, which may be assigned to a sensing enhancement by the presence of metallic Pt due to its chemical sensitization mechanism. In addition to their role in providing abundant adsorption sites , the Pt nanoparticles assist the spillover of oxygen species onto their surfaces, where the oxygen species are ionosorbed by trapping electrons from TiO_2 via the dipole-dipole interaction with the oxygen surface.[98-100] The Pt-decorated mesoporous TiO_2-based QCM sensor was also sensitive to CH_3CHO from other possible interference gases such as acetone (CH_3COCH_3), ammonia (NH_3), C_6H_6, chloromethane (CCl_4), C_2H_5OH, *n*-C_6H_{12}, and H_2O at room temperature. The sensitivity of the QCM sensor to CH_3CHO was seven times greater than that to C_2H_5OH and the QCM sensor showed a poor sensitivity to CCl_4, C_6H_6, and *n*-C_6H_{14} vapors, which was also supported by theoretical calculations.[101-102] In addition, CH_3CHO molecules were adsorbed over the Pt-decorated mesoporous TiO_2-based film rapidly within a few minutes after purging of N_2 gas inside the testing cell at room temperature. The good reversibility of the advanced QCM sensor would be very helpful for the practical use in gas sensing devices.

A mesoporous WO_3 thin film, that was fabricated by an ionic surfactant (sodium dodecyl sulfate, SDS) assisted electro-deposition method, showed a rapid QCM sensing ability to detect the contribution of the charged or uncharged species during the electrochemical processes.[103] In situ

synthesis approach for the reduction of Au nanoparticles onto a magnetic mesoporous $CoFe_2O_4$ nanostructure (Au-MMNs) and the Au-MMNs based QCM sensor showed a good conjugation capability toward biomolecules.[104] A Pearson's hard and soft acid and base (HSABs) theory was employed for the successful synthesis of urchin-like hollow sphere Zn_2SnO_4/SnO_2 by a two-step hydrothermal synthesis process.[105] The Au electrode of QCM was coated with a dispersion of the Zn_2SnO_4/SnO_2 hollow spheres in *N*,*N*,-dimethylformamide (DMF) followed by spin-coating of polyvinylidene fluoride (PVDF) over the surface of the well-dried Zn_2SnO_4/SnO_2 coated QCM electrode. The frequency of the QCM sensor cell was changed immediately after adsorption of 60 ppm dimethyl methylphosphonate (DMMP) due to the interaction between oxygen atoms of DMMP and hydrogen atoms of PVDF. Crystalline ZnO and CeO_2/ZnO nanofibrous mats can be manufactured by an electrospinning of metal salt(s) and poly(vinyl alcohol) in aqueous solution and subsequently deposited over the Au electrode of QCM.[106] After calcination for 5 h at 500 °C in air, the sensing characteristics of both ZnO and CeO_2/ZnO based QCM sensor were investigated toward some VOCs such as dichloromethane (CH_2Cl_2), C_2H_5OH, C_6H_6, and propanol (*n*-C_3H_7OH). A ZnO nanowires coated QCM sensor was chemically modified by alkyl-thiol molecules with various carbon chain lengths (C_0-C_{12}, **Figure 5A**).[107] The SEM images showed the morphology of the ZnO nanowires with the average length was approximately 2 μm (**Figure 5B**) and the peak intensity of C_{1S} was directly proportional to the carbon chain length of the alkyl-thiols (**Figure 5C**). Eventually, the experimental results revealed the significant potential application of the prepared QCM sensor for analyzing the impact dynamics of water droplets.

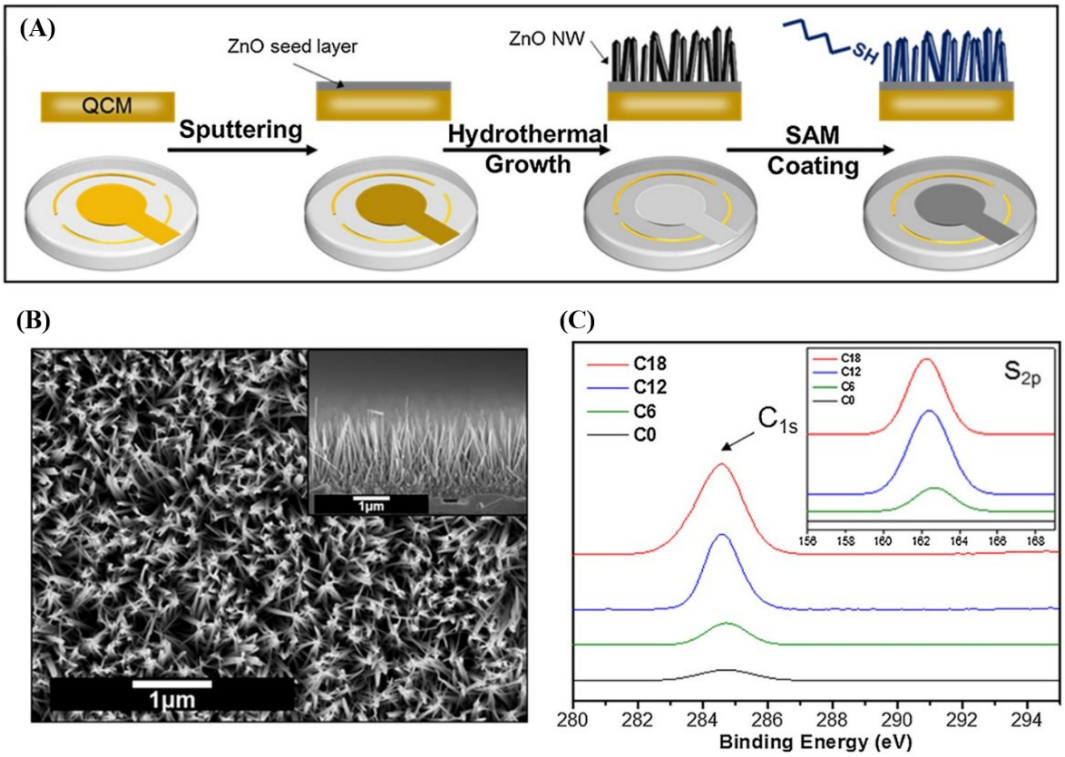

Figure 5. (A) Schematic illustration of the preparation procedure for ZnO nanowires with various surface energies on a quartz crystal through the hydrothermal synthesis and surface modification. (B) top-view SEM image of ZnO nanowires (inset: side-view SEM image). and (C) C1s XPS spectra from ZnO nanowire-grown surfaces treated with various alkyl-thiols. Inset shows S_{2p} XPS spectra. Adapted with permission.[107] Copyright 2018, ElsevierB.V.

2.1.3. Mesoporous carbon materials

A cobalt-containing mesoporous carbon based material (Co-MPC) was directly synthesized from resol in the presence of cobalt acetate through a soft-template technique using Pluronic F127 and the Co species catalyzed a graphitization of the frameworks.[108] The Co-MPC coated QCM sensor showed a better sensing affinity towards C_6H_6 and $C_6H_5CH_3$ than C_6H_{12} and other vapors. Carbon-based materials have been widely utilized as commercially

available, low-cost adsorbents so far, being potential for improving the sensing property of the QCM devices with their structural designs in nanometer scale. A layer-by-layer (LbL) assembly method for fabricating a mesoporous carbon, CMK-3, over the Au electrode of QCM with a polyelectrolyte as the binder was successfully applied for improving the sensing property of some nonionic molecules including tannic acid, catechin and caffeine (**Figure 6A**).[109] According to the effective π-π and/or hydrophobic interaction with the guest molecules, the CMK-3 LbL film coated QCM sensor exhibited a high sensitivity and selectivity. Another LbL assembly method was reported for the synthesis of dual-pore carbon capsules as an advanced QCM sensor useful for adsorption of aromatic compounds in vapor phase at ng-scale.[110] The carbon capsules with uniform pore width (4.3 nm) and high BET surface area (918 m^2 g^{-1}) were prepared by utilizing the zeolite crystals as a hard template (**Figure 6B**). The carbon capsule LbL films coated QCM sensor showed a more effective adsorption of C_6H_6 vapor almost 5 times higher than that of *c*-C_6H_{12}, being related to importance in the π-π interaction for the adsorption of aromatic volatiles.

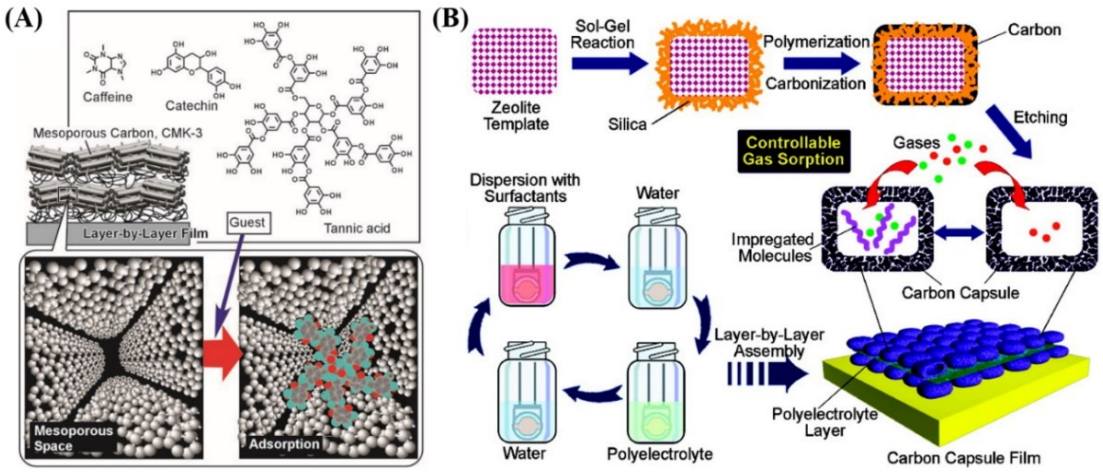

Figure 6. (A) The LbL assembly of the mesoporous carbon CMK-3 and the cooperative adsorption of guest molecules into a mesopore. Adapted with permission.[109] Copyright 2008, Wiley-VCH Verlag GmbH & Co. KGaA. (B) The schematic illustration of the construction of the carbon capsules and the LbL process of the carbon capsule film. Adapted with permission.[110] Copyright 2009, American Chemical Society.

The affinity of the carbon capsules was carefully investigated for some guest molecules having a wide variety of functional groups, such as H_2O, acetic acid (CH_3COOH), $NH_3 \cdot H_2O$, butylamine ($C_4H_9NH_2$), pyridine (C_5H_5N), and aniline ($C_6H_5NH_2$).[110] A simple photo-induced method was much interesting for the synthesis of carboxyl (-COOH) decorated ordered carbon films having meso- and macropores in the presence of uniform PS beads with various diameters as hard templates.[111] The ordered carbon-based materials with -COOH groups were prepared by a facile ozone treatment without any environmentally hazardous oxidizing agents. Because of the selective adsorption ability for volatiles, a porous carbon film coated QCM sensor was fabricated for the detection of various guest molecules such as $C_6H_5CH_3$, $C_6H_5NH_2$, *n*-C_6H_{14}, NH_3, and CH_3COOH. Interestingly, after

photo-functionalizing the porous carbon with -COOH, the porous carbon films showed a high adsorption ability to $C_6H_5NH_2$ due to the acid-base interaction with the -NH_2 groups from $C_6H_5NH_2$, in addition to the hydrophobic π-π interaction between $C_6H_5NH_2$ molecules and π bonds at the surface of the carbon-based materials.

A hierarchically porous carbon nitride (CN) coated QCM resonator showed a different adsorption performances towards various volatiles such as $C_6H_5CH_3$, *c*-C_6H_{12}, ethyl acetate ($CH_3COOC_2H_5$), *n*-C_3H_7OH, CH_3COCH_3, CH_3COOH, and $C_6H_5NH_2$.[112] The hierarchically porous CN film was synthesized using both triblock copolymer (e.g., Pluronic P123) and uniform PS spheres as the dual templates. In particular, the CN films exhibited the highest affinity towards CH_3COOH with the adsorptive equilibrium amount nearly six times larger than that of $C_6H_5NH_2$, being attributed to the presence of some basic nitrogen groups like NH_2, NH, and N sites in the CN frameworks. As a "Photo Switch Sensor", the selectivity of the CN film can be easily reversed under the UV light irradiation. The CN films showed the aforementioned high affinity towards CH_3COOH without UV irradiation and a reversible selectivity towards $C_6H_5NH_2$ under flashing with UV light in oxygen, since the UV irradiation can generate -COOH groups in the CN frameworks.[111] In addition, a carbon nanocage (CNC) embedded nanofibrous film modified QCM sensor (**Figure 7A**) was very helpful for a selective adsorption of aromatic amines than NH_3, H_2O, C_6H_6, and other compounds (**Figure 7B**).[113] The QCM sensor was fabricated by coating a cast film of poly(methyl methacrylate) (PMMA) solution containing CNC (CNC/PMMA) over the electrode of QCM. The CNC embedded nanofibrous film featured with long durability, high throughput, and low cost can be employed for the analysis of aromatic amines from the breath gas samples prior to contraction of cancer as well as such amines in the workplaces.

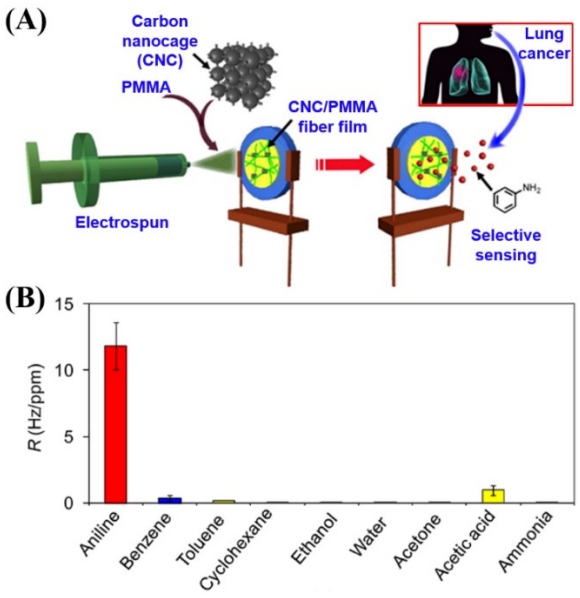

Figure 7. (A) Schematic illustration of the Carbon nanocage-embedded nanofibrous film-based QCM sensor and the selective sensing aniline vapor from the breath gas of lung cancer. (B) The selective adsorption selectivity of the QCM sensor for aromatic amines, water, benzene, ammonia and other chemical species. Adapted with permission.[113] Copyright 2013, American Chemical Society.

A QCM sensor modified with a nitrogen-doped mesoporous carbon (N-CMK-3) showed various adsorption abilities towards diverse analytes, including $C_6H_5CH_3$, $C_6H_5NH_2$, NH_3, C_2H_5OH, CH_3COOH, and so on.[114] The N-CMK-3 type materials were synthesized through a nanocasting of a gelatin biomolecule as the precursor into the mesopores of SBA-15 as the hard template and showed the strongest basicity helpful for a good adsorption selectivity to CH_3COOH among other species. A series of mesoporous materials with high C/N ratio were also prepared successfully by a nano-hard-templating method.[115] Since this material was constructed at a temperature lower than 450 °C, the considerable amount of nitrogen atoms

can be preserved very well in the carbon-based frameworks. Thus, QCM sensors modified with the high C/N materials were utilized for adsorption of both basic and acidic volatiles. Interestingly, the high C/N material with larger pore width exhibited a better adsorption ability to acidic species, e.g., formic acid (HCOOH) due to from the presence of a plenty of weak basic sites in the frameworks.

2.2. Carbon-based nanomaterials

2.2.1. Carbon nanotubes (CNTs)

CNTs have been developed for the modification of the QCM electrode and the minor changes in conductivity were amplified to the vibrational frequency signal in the modified QCM sensors.[116] The fabricated QCM electrode possessed an excellent robustness and stability, which successfully employed for sensing of various targets such as VOCs, aldehydes and amines. Functionalization of CNTs is also promising to impart QCM sensors with good functional surface features which cannot be fulfilled using pristine CNTs. Therefore, the functionalized CNTs can be acted as a platform to construct advanced QCM sensors for the adsorption of some vapors such as C_6H_6 and xylene ($C_6H_4(CH_3)_2$).[117] Furthermore, many interactions between functionalized CNTs modified substrate and analytes would lead to different behaviors and responses. For instance, a single-wall CNT coated QCM sensor can act as a sensitive real-time platform for the analysis of Cymbidium mosaic potexvirus (CymMV) in the infected orchid leaves.[118] A fast, economical, and ultra-sensitive detection with a comparable sensitivity was realized as the enzyme-linked immunosorbent assay (ELISA) by using the CNT-based QCM method.

2.2.2. Graphene materials

Graphene is as a new generation of porous materials due to its diverse remarkable characteristics such as high surface area, rich stacking π-electrons, and homogeneous thickness.[119-123] A LbL assembly technique was applied for the construction of a layered graphene/ionic liquid (G-IL) composite over the QCM substrate for sensing diverse vapors.[124] The G-IL-based QCM sensor, inside the well-defined π-electron-rich nanospace, exhibited a higher adsorption captivity for toxic aromatic hydrocarbons than those for their aliphatic analogues. The higher selectivity (>10 times) of C_6H_6 vapor was achieved than *c*-C_6H_{12} even in the case to detect organic molecules having similar molecular sizes and vapor pressures. The G-IL composite film also showed the potential environmental application by the capture of CO_2. A graphene oxide (GO) modified QCM humidity sensor, which exhibited a good adsorption reversibility with a rapid response and recovery time (less than 20 s and 3 s, respectively), was successfully fabricated, due to the high hydrophilic nature and large surface area of GO.[125]

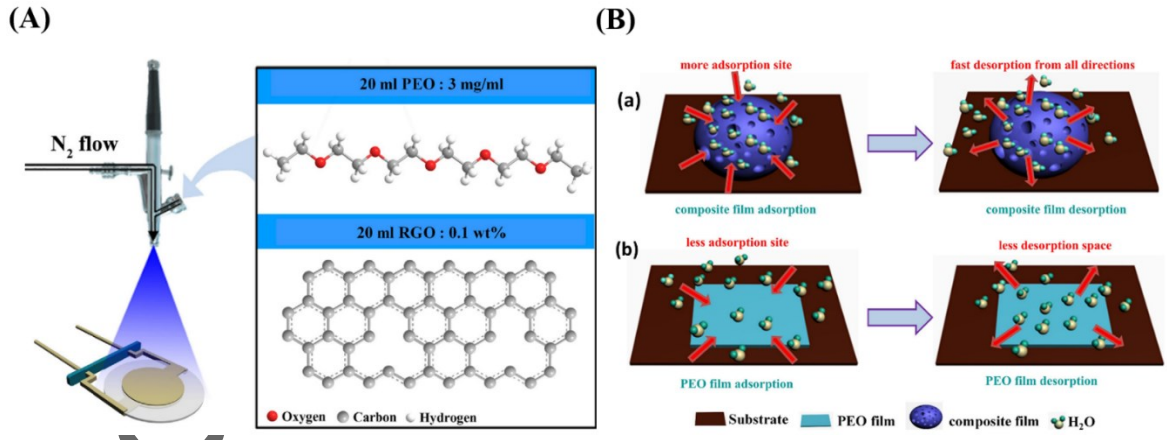

Figure 8. (A) Schematic illustration of the RGO-PEO composite film deposition by the spray method. (B) Illustration of the humidity mechanism of the pure PEO film (a) and the RGO-PEO composite film (b) based QCM sensors. Adapted with permission.[126] Copyright 2018, Elsevier B.V.

Pure graphene surfaces do not allow adsorption of H_2O molecules because of the weak interaction, which limits the further application of graphene in the humidity sensors. Because a poly(ethylene oxide)-reduced GO (PEO-rGO) composite with high crystallinity provided a great possibility for the sensitive detection of humidity,[126] the PEO-rGO composite film modified QCM sensor was fabricated by a spray method (**Figure 8A**). Compared with a pure PEO film based QCM sensor, the PEO-rGO composite one showed rapid response/recovery (11s/7s at 90% RH) at 84% RH and high sensitivity, which might be contributed to the surface roughness of the PEO-rGO composite film with a large surface-to-volume ratio and abundant adsorption/desorption sites with long term stability (**Figure 8B**). A facile QCM biosensor was designed through a GO-biotin-based sandwich immunoassay method (**Figure 9**) based on the irreversible adsorption of GO to a standard Au-coated QCM chip.[127] This highly effective method just needs a few simple flow-based steps, avoiding the conventional time-consuming chemical pre-functionalization strategy. The GO-modified QCM sensor showed the advantages of on-line, rapid, and highly sensitive in the analysis of an antigen target.

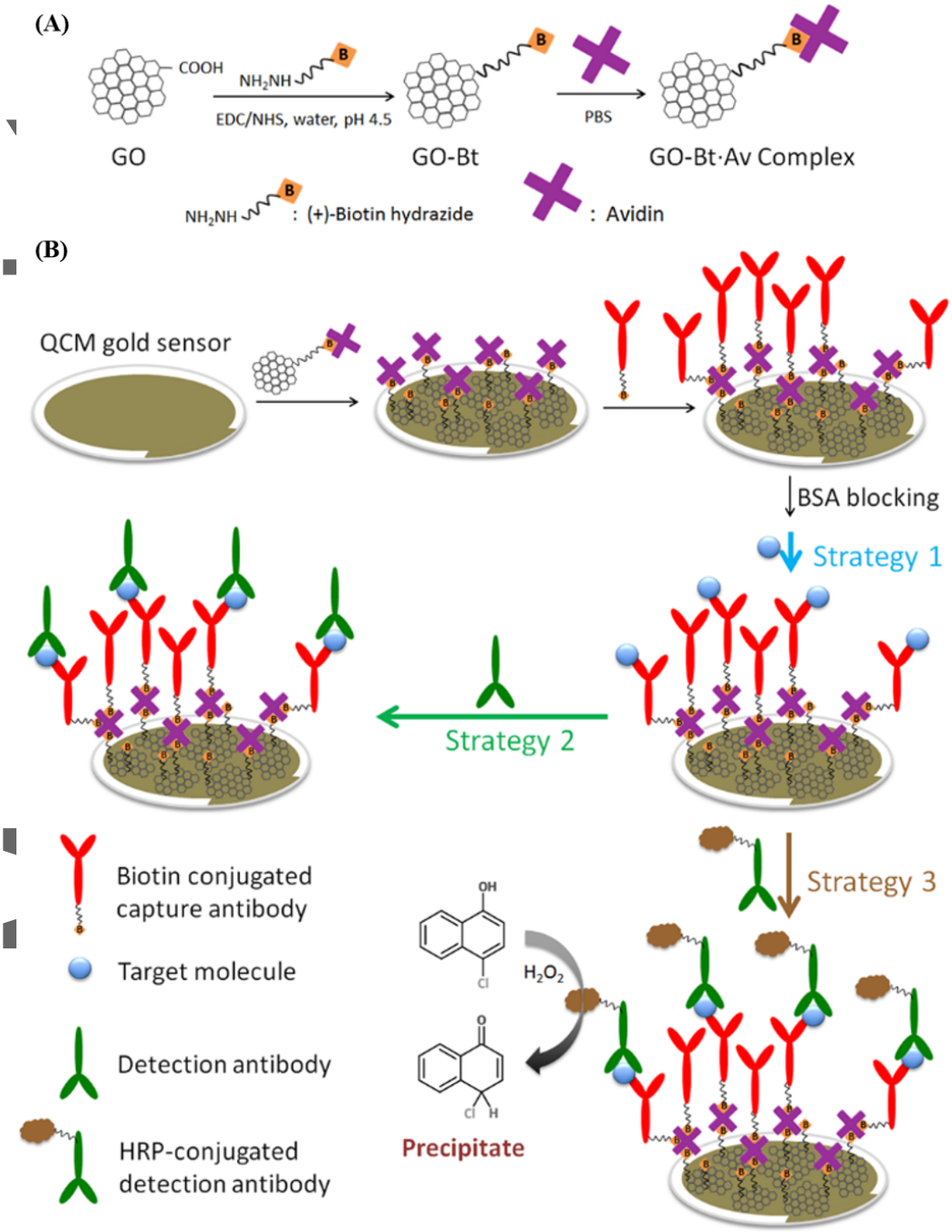

Figure 9. (A) The reaction scheme to form biotinylated graphene oxide (GO-Bt) and graphene oxide·avidin (GO-Bt·Av) complex. (B) Schematic diagram of the flow-based fabrication of QCM-based immunosensor and the three tested strategies for antigen quantification. Adapted with permission.[127] Copyright 2016, American Chemical Society.

2.3. Porous coordination polymers (PCPs)-based materials

2.3.1. Metal-organic frameworks (MOFs)

In the past decades, MOFs have been extensively served as the precursors for the construction of a considerable nanoporous materials, ranging from carbon- to metal-based nanomaterials (carbide, oxide, chalcogenide, phosphide, etc.). The transformations from MOFs into carbon- or metal-based nanoporous materials are stimulated by the porous architectures of MOFs and their attractive components which include diverse metal ions/clusters and abundant organic linkers.[128] The significant porosity of MOFs and MOFs-derived nanomaterials have allowed inclusion of large molecules into the nanospaces and enhancement of sensing applications by using the high surface areas.[129-132] Construction of surface-mounted MOFs (SURMOFs) has aroused a growing interest and a considerable of techniques have been developed for the MOF coatings onto the QCM substrate. For the preparation of thinner MOF films, the liquid-phase epitaxy (LPE) method has been utilized by immersing the substrate in the reaction mixture of the MOFs suitable for creating corresponding films with the adjustable thickness from nm- to mm-levels.[133] In this technique, diverse SURMOFs can be fabricated directly over self-assembled monolayers (SAM) of organic molecules.[134-135] The SURMOFs-coated QCM devices have been demonstrated as an advanced chemical sensor for the studying and characterizing of the mass transfer processes of the MOFs.[136]

MOFs with different structures have been also applied as the gas sensor for hydrogen (H_2), oxygen (O_2), CO_2, methanol (CH_3OH), C_2H_5OH, propane (C_3H_8), NO, and H_2O in the atmosphere mixture.[137] For instance, a zeolitic-imidazolate framework-8 (ZIF-8) was modified onto the QCM device for the detection of methane (CH_4) and CO_2.[138] The ZIF-8 layer coated QCM sensor achieved a relatively higher sensitivity of CO_2 rather than CH_4 since its higher molecular weight. Besides, this highly stabile QCM device can be also served

as a reversible and repeatable gas sensor. A MOF-199 (HKUST-1, $Cu_3(btc)_2$, btc; 1,3,5-benzenetricarboxylate) thin layer was integrated over a microcantilever sensor surface for the detection of H_2O, CH_3OH, and C_2H_5OH vapors.[139] The strain changes were induced on the cantilever through adsorption and desorption of the vapors at the interface between the cantilever surface and the MOF film, which was detected by the piezoresistive sensor. Since HKUST-1 possessed hydrate and dehydrate forms with two exchangeable coordination sites, which can be easily occupied by the H_2O molecules. The dehydrated HKUST-1-coated sensor exhibited a higher selectivity towards CO_2 and alcohols rather than O_2 and N_2, indicating that HKUST-1 was potentially useful for a breath analysis. The piezoelectric microcantilever coated with HKUST-1 was active for the detection of humidity and hydrocarbon gases.[140] The HKUST-1 coated sensors showed different degrees of adsorption and desorption discrimination of various VOCs, e.g., CH_3OH, isopropanol (i-C_3H_7OH), H_2O and CH_3COCH_3 upon their response time. A similar HKUST-1 coated QCM sensor was also synthesized for the relative humidity sensing and showed a higher humidity sensitivity due to its high adsorption energy.[141]

Through developing a controlled pressure and temperature QCM-based system, adsorption properties towards CO_2, CH_4 and N_2 was investigated by using Cu-MOF (Cu-hfipbb) and ZIF-90.[142] The adsorption order was $CO_2 > CH_4 > N_2$ in both MOFs. The adsorption kinetics of Cu-hfipbb was consistent with a single-site Langmuir model, corresponding to its porous architecture composed of one-dimensional (1-D) nanochannels but without remarkable cage-like structure. However, in the case of ZIF-90, there are considerable large porous cages in three-dimensional (3-D) structures, resulting in the large deviations from Langmuir adsorption. The detection of VOCs was studied by employing the MOFs thin films coated microcantilever sensors.[143] As shown in **Figure 10**, two

-COOH terminated MOFs layers were self-assembled onto the Au electrode of QCM to fabricate sensor platforms. Due to the molecular sieving effects in the regulated nanospace of the MOFs, the $Cu_3(BTC)_2$ layer-coated QCM sensor showed different adsorption abilities towards various VOCs, in particular, $C_6H_5CH_3$ at a concentration of 1 ppm. The adsorption sensitivity of $Zn_4O(BDC)_3$ coated QCM sensor was lower than that of the $Cu_3(BTC)_2$ sensor to $C_6H_5CH_3$ since the presence of larger pore and aperture sizes in $Zn_4O(BDC)_3$ which result in a low size-selective effect for VOCs.

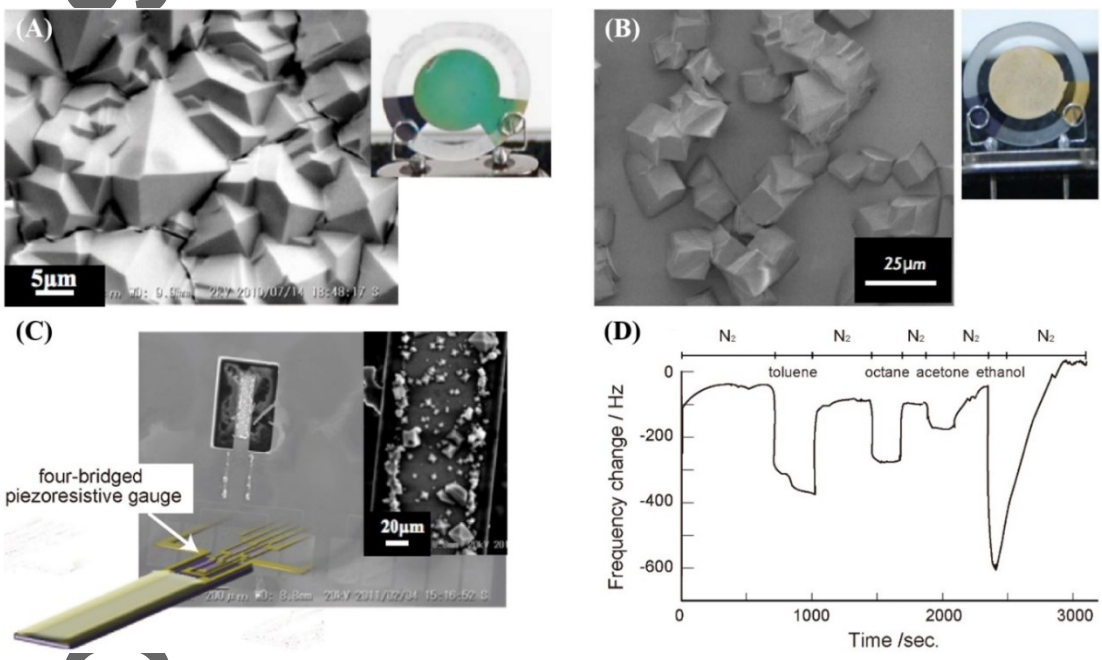

Figure 10. (a) SEM image and photograph of $Cu_3(BTC)_2$ thin film grown from COOH-terminated SAM on gold electrode of QCM, (b) SEM image and photograph of $Zn_4O(BDC)_3$ thin film grown from COOH-terminated SAM on gold electrode of QCM. (c) and (d) SEM image and photograph of $Cu_3(BTC)_2$ thin film grown from COOH-terminated SAM on gold electrode of microcantilever resonator and frequency response of $Cu_3(BTC)_2$ film on the microcantilever resonator upon exposure to 100 ppm toluene, *n*-octane, acetone, and ethanol vapors. Adapted with permission.[143] Copyright 2014, Springer Nature Publishing AG.

Another fascinating method for the construction of MOFs thin films coated QCM sensors was the Langmuir-Blodgett (LB) approach, which permitted the deposition processes happened at the air-liquid interface of monolayers. These monolayers, composed of nanoparticles, polymers or organic molecules, can be directly deposited onto various substrates, e.g., quartz, glass, and silicon, without any functionalization.[144-145] A three-dimensional (2-D) binary Janus PCP was fabricated by depositing PCPs over the QCM substrate by employing the LB method.[130] The heterogeneous PCPs were utilized as the QCM coatings for the sensing of VOCs. A mixed LB film, combined NH_2-MIL-88B(Fe) with a polyimide was designed to gain a homogeneous ultrathin MOF-polymer film, which motivated the further synthesis of ultrathin MOF-based films.[146] The MIL-101(Cr) layers were deposited over different substrates (quartz, glass and silicone) by using a LB method.[147] MIL-101(Cr), with the size of approximately 50 nm, was synthesized and characterized by using UV-vis, SEM and XRD. Behenic acid (BA), a generally known surfactant, was utilized for stabilizing the Langmuir layers with the reduction of the stress forces and prevention of aggregations from MIL-101 nanoparticles at the air-water interface. The MIL-101 coated QCM sensor was applied for obtaining adsorption isotherms of CO_2 on the LB film at 100 kPa as the accurate adsorption value, being similar to those gained by the conventional adsorption technique which usually need of much more amount of MOFs.

An activated 3-D calcium spirobifluorene (Ca-SBF)-based MOF with regular nanopores and medium surface area was employed for the fabrication of QCM sensor toward VOCs including $C_6H_5CH_3$, C_2H_5OH, CH_3COCH_3 and C_6H_6.[148] Due to a well-matching of the pore aperture of Ca-SBF-based MOF with the diameter of $C_6H_5CH_3$, a selective response to $C_6H_5CH_3$ vapor was obtained. A ultrathin drop-cast, LB and Langmuir-Schaefer (LS) films of microporous aluminum (Al)

tricarboxylate MOF (MIL-96(Al)) was fabricated for CO_2 adsorption study by the QCM technique using very small MOF quantities.[149] Adsorption behavior of CO_2 was controlled by the MIL-96(Al) film fabrication method in addition to its storage conditions and the solvent used in suspension preparation and its desorption was done at the room temperature by the flow of an inert gas. The MIL-96(Al) LB film exhibited a good stability after 15 cycles of CO_2 adsorption/desorption. Another method was described for detecting C_5H_5N vapor,[150] using the QCM sensor coated with a nanoscale MOF (N-MOF), Al(OH)(1,4-NDC). Adsorption capacity of N-MOF-coated QCM sensor was improved by using CH_2Cl_2 instead of DMF to homogeneously disperse N-MOF onto the Au electrode. The N-MOF-coated sensor showed a high selectivity, good reproducibility, and long-term stability for sensing of C_5H_5N. The adsorption mechanism of the QCM sensor towards C_5H_5N was studied by a van der Waals-modified density functional theory (DFT) calculation.

2.3.2. Prussian blue and its analogues

Prussian Blue (PB) and PB analogues (PBAs) represent a well-known class of coordination polymers (CPs), built form metal cations M^{n+} nodes bridged with cyanide ligands (M^{2+}-CN-M^{3+}).[151] In the sense of applications, PB and PBAs are potential for a wide variety of applications such as electrocatalysis, electrochromism, and magnetism and excellent adsorbents for trace analysis of small molecules and ions, particularly for their high nanoporosity, high surface area, high performances, and environmental safety.[152-160] Due to their excellent removal ability for Cs cation (Cs^+), PB has been commercialized medicinally for patients who suffer from internal contamination of radioactive Cs^+ from gastrointestinal tract of animals because of its strong affinity for Cs^+.[161]

A facile method to synthesize water-insoluble PB nanoparticles was demonstrated with the formation of diverse particle sizes ranging from a few dozen nanometres to submicrometres called

as small-sized, medium-sized, and large-sized PB particles.[162] The PB having diverse particle sizes was designed as an advanced QCM sensor for studying the adsorption uptake of Cs^+. A fast and sensitive sensor was realized in a case using the medium-sized PB particles, which exhibited Cs^+ uptake of more than 2 times higher than that for the large-sized ones as a result of the high surface area. The Cs^+ adsorption mechanism was investigated by the uptake of Cs^+ into the nanocavities of PB, rather than ion-exchange mechanism due to the absence of K^+. The PB particle size was significant for optimizing the Cs^+ adsorption rate. A different synthetic route was developed for preparing a high surface area single crystalline PB particles with interior hollow cavities (up to 330 $m^2\ g^{-1}$) via a controlled self-etching of PB cubes. [161] The structure characteristics in turn were very unique in the environmental clean-up of radionuclide ^{137}Cs when thin layers of PB were integrated with a QCM sensor with the aid of Nafion binder. The hollow nanocavities afforded a huge adsorption uptake for Cs^+ from its aqueous solution.

For further enhanced Cs^+ adsorption capability, new single crystalline hollow PBA nanocubes, composed of pairs of Co-Fe, Ni-Fe, and Mn-Fe were explored by a simple chemical etching process by using polyvinylpyrrolidone (PVP) as a protecting agents as the ideal candidate for the removal of Cs^+.[163] According to the high surface area caused by the hollow nanocavities and highly crystalline microporous structures, the PBA, Ni-Fe hollow nanocubes exhibited a good adsorption uptake of Cs^+ compared with its corresponding analogue which can be confirmed by the QCM technique. In addition, the high-surface-area PB nanoparticles was successfully dispersed in a poly(*N*-isopropylacrylamide) (PNIPA) hydrogel, which would be consequently useful for the remediation of radioactive Cs.[164] The adsorption uptake of Cs^+ was studied by using QCM sensors coated with the PB nanoparticles where the loading amount of the PB nanoparticles were estimated as 11.90 $\mu g\ cm^{-2}$. By the increase in the effective surface area of the PB nanoparticles, the higher

affinity of the PB nanoparticles toward Cs^+ was useful for a large Cs^+ uptake of 191.4 mg g^{-1}, being almost 6 times higher than that in a case using commercial PB particles (38.8 mg g^{-1}).

2.3.3. MOF-derived nanoporous carbons

Sacrificial utilizations of MOFs for obtaining functional nanoporous materials with enhanced properties are the state-of-the-art technique that integrates MOF-derived nanomaterials on conductive substrate and electrode having flexibilities, including carbon cloths and fibers/textiles, QCM, etc., which may provide an excellent opportunity for creating commercial flexible supercapacitors, batteries and industrially attractive in situ detection systems. For example, MOFs have been utilized as precursors for the synthesis of nanoporous carbon (NPC) based materials by carbonizing MOFs with a secondary carbon precursor into their cavities.[165-167] For a high specificity of the interaction with target substances, the chemical design of nanostructures and functionalities is quite crucial for fabricating QCM sensors showing high selectivity. ZIF-8 derived NPCs prepared by direct carbonization of the ZIF-8 crystals without additional carbon precursors were a promising adsorbent for effective removal toxic Cu^{2+} from a potable water.[168] The NPC particles showed an impressive adsorption capacity of Cu^{2+} compared with other carbonaceous adsorbents. Combing the unique properties, such as high surface area, high nanoporosity, and highly graphitic (sp^2) carbon frameworks, along with the co-existence of surface hydroxyl (-OH) and carboxylic (-COOH)groups, the ZIF-8 derived NPCs were useful for a fast ion diffusion of Cu^{2+} with the high adsorption capability , possibly due to the mechanisms of $\equiv C\text{-}OH + Cu^{2+} = \equiv C\text{-}OCu^+ + H^+$ and $-COOH + Cu^{2+} = -COOCu^+ + H^+$.[168] Thus, the adsorption efficiency of ZIF-8 derived NPCs for Cu^{2+} was linearly increased by decreasing the H^+ concentration in the medium.

A facile and scalable method was also proposed for exclusively synthesizing varieties of MOFs-derived NPCs confined metal nanoparticles with a wide range of compositions. In this context, magnetic Co NPs were successfully confined in MOFs-derived NPC particles (named as Co/NPC particles) by a one-step carbonization of ZIF-67 crystals.[169] The highly crystalline and well-dispersed fine Co NPs (up to nearly 50 mass%) confined in NPC matrices were very helpful for graphitization of derivative carbon based frameworks with retention of a porosity, realizing an excellent adsorption performance of toxic methylene blue (MB) dye molecules. From the QCM study, the Co/NPC-modified electrode showed an impressive adsorption capacity for the MB molecules (509 mg g^{-1}) calculated by using the Sauerbrey's equation (Eq. 1), being in good agreement with that measured by UV-Vis. The enhanced MB adsorption (almost 10 times higher than that observed for an activated carbon) was attributed to the high nanoporosity with an open pore texture. High graphitization degree of sp^2-carbon species also provided more adsorption sites effective for interaction with MB molecules through π-π bonds. In a sense of the practical application, the Co/NPC particles showed a good reversibility of almost 86 mass%.

An alternative simple one-step pathway for synthesizing NPC with an extreme high surface area (5500 m^2 g^{-1}) and large pore volume (4.4 cm^3 g^{-1}) that were derived by a direct carbonization of an Al-based PCP (Al-PCP, (Al(OH)(1,4-NDC)·$2H_2O$) [170] (**Figure 11**). The highly graphitic material having outstanding porosity was drop-coated over the electrode of QCM after assembling polyion polydiallyldimethylammonium (PDDA) chloride and sodium polystyrene sulfonate (PDDA/PSS) binder layers. A large uptake with very high sensing affinity for C_6H_6 vapors was clearly observed with an excellent repeatability, which was attributed to the extreme high surface area and nanoporosity. In addition, the sensor also showed the higher selectivity for aromatic hydrocarbons (e.g., C_6H_6 and $C_6H_5CH_3$) than those for aliphatic ones (*n*-C_6H_{14} and *c*-C_6H_{12}) as a result of π-π interactions between aromatic rings and graphitic sp^2 carbon frameworks.[109, 124] In addition, the designed QCM sensor

coated with ZIF-8 derived NPC particles in the presence of Nafion binder also showed an improved sensor response for $C_6H_5CH_3$ vapors.[171] Particle sizes of ZIF-8 derived NPCs was controllable in the range from nm to μm scale with the retention of the original shape of parent ZIF-8 crystals. Although the surface area of large- and small-sized ZIF-8 derived NPC particles was useful for large adsorption uptakes of $C_6H_5CH_3$ molecules, the small-sized NPCs might be helped for the uptake of more $C_6H_5CH_3$ molecules into the ZIF-8 derived NPCs over the entire QCM electrode.

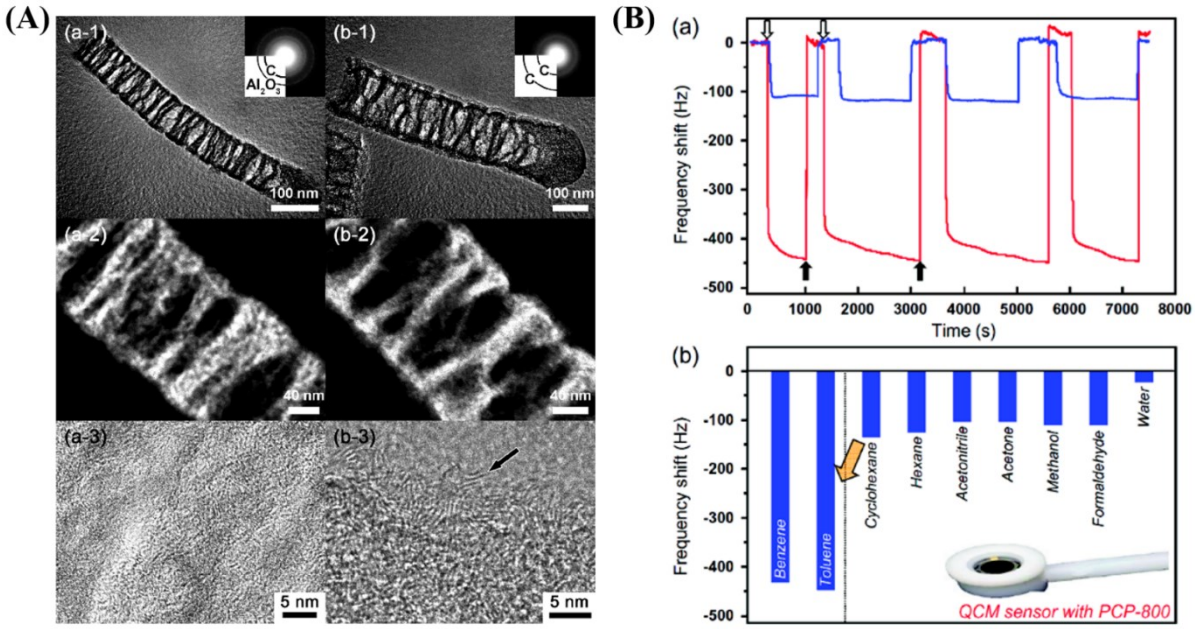

Figure 11. (A) Bright- and dark-field TEM images of Al-PCP calcined at 800 °C (a) before and (b) after washing with HF. The inset is the corresponding ED pattern. (a-3) and (b-3) High resolution TEM images of Al-PCP calcined at 800 °C before and after washing by HF, respectively. The graphitic sheets are indicated by arrow. (B-a) QCM frequency shifts upon benzene adsorption into (red-line) PCP-800 film and (blue-line) active carbon film. The changes of the QCM frequency shifts are examined through alternate exposure (open arrows) and removal (filled arrows) of the benzene molecules. (b) Summary of QCM frequency shifts of PCP-800 film caused by exposure to various vaporized gases. These QCM frequency shifts are recorded 500 s after the PCP-800 films are exposed to vapors. Adapted with permission.[172] Copyright 2012, American Chemical Society.

2.4. Zeolites and related materials

Zeolites and related materials were extensively studied to remove environmental waste effluents at the low-level of concentration ranges.[173] Adsorption of toxic metal cations into zeolite cavities occurs with ion-exchange reactions because negative charges of zeolite (aluminosilicate) frameworks have to be balanced by chemically exchangeable cations in solutions. In addition to reasonable prices of zeolites, their molecular sieving effects, excellent ion-exchange and selectivity, zeolite coated QCM sensors were extensively studied towards the development of gas sensing and toxic ion uptake.[167] Zeolites such as LTA, BEA, MFI, FAU, CHA were utilized for the sensing of humidity and VOCs like C_2H_5OH, *n*-C_3H_7OH, isooctane (*i*-C_8H_{18}), C_5H_5N, and perfluorotributylamine ($N(C_4F_9)_3$.[174-176] Considering the pore size, the BEA type zeolite exhibited a higher affinity to relatively large organic molecules such as pentane (*n*-C_5H_{12}), *n*-C_6H_{14} and *c*-C_6H_{12}), although no selectivity was observed among them, while the LTA one showed a selective response to H_2O vapors. Zeolite (e.g., zeolite A, silicalite-1 and sodalite) coated QCM electrodes was also developed for sensing NO, SO_2 and humidity.[177-178] The sodalite (SOD) coated QCM device was promising to discriminate humidity even in the presence of other gases because of poor responses towards NO and SO_2 gases. Acoustic QCM sensors modified with zeolites, include silver-exchanged MFI type one,[179] principle component analysis of multiple-QCM sensors coated with LTA, MFI, and SOD were reported for a selective response to CH_3COCH_3 in diabetic's breath in ppm range and detection of NO/SO_2 mixture, respectively.[178]

Colloidal zeolites with MFI and LTA type framework architectures were synthesized and used as building blocks for the assembly of porous films on an isocyanate-SAM functionalized Au electrode of a QCM oscillator.[180] The molecularly selective sensing behavior of the zeolite-coated QCM devices were demonstrated by evaluating the adsorption isotherms of *n*- and *i*-butane (C_4H_{10}). Ji and

co-workers[181] prepared ZSM-5 and Cu-ZSM-5 containing various percentages of Cu^{2+} were prepared and fabricated as sensitive QCM films by a self-assembly method. In particular, Cu-ZSM-5 demonstrated a good selectivity and high sensitivity to DMMP vapor. Zeolite A nanoparticles prepared by a simple post-milling recrystallization was reported for uptake of Cs^+.[182] The nanometer-sized zeolite A accommodated much Cs^+ uptake (422 mg g^{-1}) in comparison with micrometer-sized one (168 mg g^{-1}) due to its high surface area, which would be promising for radioactive Cs recovery from polluted effluents. The ion-exchange ratio of Na^+ in the sodalite cage to Cs^+ was estimated to be 45%, which may be attributed to the small opening of the sodalite cage to prevent smooth diffusion of Cs^+. The Cs adsorption kinetics was further studied using a real-time monitoring of ΔF of QCM. From theoretical calculations (Eq. 8), the estimated rate of uptake (k) of Cs^+ form the gradient of the kinetic plot of $\ln(\Delta F_t/\Delta F_\infty)$ versus time (t) clearly showed that adsorption of Cs^+ into the nanometer-sized zeolite A was 1.4 times faster than that into micrometer-sized one.

3. Future prospects

Recent development of the QCM sensing technique has been powered by conceptual simplicity, low cost, ease of modification, ruggedness, chemical inertness of electrode, reliability, sensitivity, availability of piezoelectric transducers, and economic efficiency of its technical products. The frequency measurement outputs are very precise and dealing with the associated electronics is fairly simple and the QCM sensor can respond to a wide range of stimuli such as temperature variations and pH shifts as well as injected chemicals and biomaterials. To design advanced detection systems having high sensitivity, introduction of advanced nanostructured materials to the QCM system is very useful for various applications in science and technology disciplines. To develop highly efficient adsorbents, materials nanoarchitectonics may be one of the answers in the future for their intrinsic properties such as high surface area, large pore volume, tunable pore size, and high stability.

Interconnected pore wall surfaces can be in turn modified or functionalized with active function groups. Such unique properties meet the future sensor requirements, not only providing huge spaces for accommodating large guest species but also enabling the selective guest binding and enrichment through active functionalities.

The QCM-based non-gravimetric technique has provided valuable studies for the qualitative and quantitative investigations of molecular recognitions using advanced nanostructured materials. Although miniaturized QCM microanalytical technique is promising for future studying the guest adsorption and diffusion processes, further progress is needed for the development of appropriate approaches for reliable and routine sample preparation onto the QCM electrode. The present results and forthcoming studies are expected to be analytically useful in validating and parametrizing molecular models for studying adsorption process occurred in nanoporous materials. The versatility in the synthesis of functional nanoporous materials also holds the great potential for creating molecular recognition sensors to enable selective detection/adsorption of a wide range of toxic chemicals. Encouraged by the compatibility of nanoporous materials with the piezoelectric QCM sensor, a mixture of analytes can be detected using an array of the QCM electrode functionalized with different nanoporous materials in order to take advantage of their respective chemical selectivity. The pore tunability of advanced nanoporous materials is also considered as a key advantage for designing chemical sensor arrays with a pattern recognition library for electronic nose systems.

We believe that works on the fabrication of electronic nose systems for the on-line and real-time monitoring of VOCs in ambient environments are underway in future. On-line and real-time monitoring of trace-level VOCs is quite important to allow the situational awareness for controlling exposure to health and safety risks associated with the surrounding hazard substances. Another important aspect, the detection of the VOCs generating from our bodies using

the QCM sensor technique will open a new avenue for non-invasive and fast health monitoring such as those for cancers, kidney diseases and neurodegenerative diseases that can help physicians in medical diagnosis. Surface modification of the metal electrode, for example by using self-assembled monolayer coupling agents may also be available for improving selective adhesion of nanoporous materials deposition. Yet, we have only scratched the surface of possibilities, due to the vast number of candidates like various nanoporous materials. Future researches will explore the phase space of available materials with differing pore sizes, morphology, and chemical functionality.

Acknowledgements

N.L.T. and S.Z. contributed equally to this work. This work was financially supported by the Australian Research Council (ARC) Future Fellow (FT150100479), JSPS KAKENHI (17H05393 and 17K19044), and the research fund by the Suzuken Memorial Foundation. S.Z. acknowledges the supports of the Youth Top-notch Talent Foundation of Hebei Provincial Universities (Grant No. BJ2018024). W.A.A. thanks the Cultural Affairs and Missions Sector of the Egyptian Ministry of Higher Education for financial support. T.K. also thanks the financial support by JSPS KAKENHI Grant Number 19H02805.

References

[1] P. Curie, J. Curie, *C. R. Acad. Sci.* **1880,** *91*, 294.

[2] W. P. Mason, *Piezoelectric Crystal and their Application to Ultrasonics* **1950,** *Van Nostrand, New York*.

[3] G. G. Guilbault, J. M. Jordan, E. Scheide, *CRC Crit. Rev. Anal. Chem.* **1988,** *19*, 1.

[4] C. I. Cheng, Y.-P. Chang, Y.-H. Chu, *Chem. Soc. Rev.* **2012,** *41*, 1947.

[5] A. C. Hillier, M. D. Ward, *Anal. Chem.* **1992,** *64*, 2539.

[6] G. Sauerbrey, *Z. Phys.* **1959,** *155*, 206.

[7] S. K. Vashist, P. Vashist, *J. Sensors* **2011,** *2011*, 13.

[8] R. E. Speight, M. A. Cooper, *J. Mol. Recognit.* **2012,** *25*, 451.

[9] W. H. King, *Anal. Chem.* **1964,** *36*, 1735.

[10] E. T. Watts, J. Krim, A. Widom, *Phys. Rev. B* **1990,** *41*, 3466.

[11] C. E. Reed, K. K. Kanazawa, J. H. Kaufman, *J. Appl. Phys.* **1990,** *68*, 1993.

[12] D. Johannsmann, K. Mathauer, G. Wegner, W. Knoll, *Phys. Rev. B* **1992,** *46*, 7808.

[13] M. M. Ayad, N. Salahuddin, M. A. Sheneshin, *Synthetic Met.* **2003,** *132*, 185.

[14] M. M. Ayad, A. H. Gemaey, N. Salahuddin, M. A. Shenashin, *J. Colloild Interf. Sci.* **2003,** *263*, 196.

[15] M. M. Ayad, *J. Mater. Sci.* **2003,** *22*, 1577.

[16] M. M. Ayad, A. F. Rehab, I. S. El-Hallag, W. A. Amer, *Eur. Polym. J.* **2007,** *43*, 2540.

[17] S. Bruckenstein, M. Shay, *Electrochim. Acta* **1985,** *30*, 1295.

[18] K. K. Kanazawa, J. G. G. II, *Anal. Chim. Acta* **1985,** *175*, 99.

[19] P. D. R. Schumacher, *Angew. Chem. Int. Ed.* **2010,** *29*, 329.

[20] D. A. Buttry, M. D. Ward, *Chem. Rev.* **1992,** *92*, 1355.

[21] A. L. Kipling, M. Thompson, *Anal. Chem.* **1990,** *62*, 1514.

[22] L. V. Rajakovic, B. A. Cavicvlasak, V. Ghaemmaghami, K. M. R. Kallury, A. L. Kipling, M. Thompson, *Anal. Chem.* **1991,** *63*, 615.

[23] V. Tsionsky, E. Alengoz, L. Daikhin, A. Kaverin, D. Zagidulin, E. Gileadi, *J. Electrochem. Soc.* **1995,** *143*, 2240.

[24] E. J. Calvo, C. Danilowicz, R. Etchenique, *J. Chem. Soc. Faraday Trans.* **1995,** *91*, 4083.

[25] J. Rickert, A. Brecht, W. GoPel, *Anal. Chem.* **1997,** *69*, 1441.

[26] C. C. White, J. L. Schrag, *J. Chem. Phys.* **1999,** *111*, 11192.

[27] J. Kankare, *Langmuir* **2002,** *18*, 7092.

[28] V. M. Mecea, *Anal. Lett.* **2005,** *38*, 753.

[29] P. L. Konash, G. J. Bastiaans, *Anal. Chem.* **1980,** *52*, 1929.

[30] T. Nomura, M. Okuhara, *Anal. Chim. Acta* **1982,** *142*, 281.

[31] K. Keiji Kanazawa, J. G. Gordon, *Anal. Chim. Acta* **1985,** *175*, 99.

[32] K. K. Kanazawa, J. G. Gordon, *Anal. Chem.* **1985,** *57*, 1770.

[33] Q. Kang, Q. Shen, P. Zhang, H. Wang, Y. Sun, D. Shen, *Anal. Chem.* **2018,** *90*, 2796.

[34] B. Acharya, M. A. Sidheswaran, R. Yungk, J. Krim, *Rev. Sci. Instrum.* **2017,** *88*, 025112.

[35] L. Daikhin, M. Urbakh, *Faraday Discuss.* **1997,** *107*, 27.

[36] L. Daikhin, E. Gileadi, G. Katz, V. Tsionsky, A. Michael Urbakh, D. Zagidulin, *Anal. Chem.* **2002,** *74*, 554.

[37] G. Mchale, M. I. Newton, *J. Appl. Phys.* **2004,** *95*, 373.

[38] Lubica Macakova, Eva Blomberg, P. M. Claesson, *Langmuir* **2007,** *23*, 12436.

[39] S. Sigalov, N. Shpigel, M. D. Levi, M. Feldberg, L. Daikhin, D. Aurbach, *Anal. Chem.* **2016,** *88*, 10151.

[40] O. Zybaylo, O. Shekhah, H. Wang, M. Tafipolsky, R. Schmid, D. Johannsmann, C. Wöll, *Phys. Chem. Chem. Phys.* **2010,** *12*, 8093.

[41] U. Balakrishnan, N. Ananthi, S. T. Selvan, R. Pal, K. Ariga, S. Velmathi, A. Vinu, *Chem. Asian J.* **2010,** *5*, 897.

[42] K. Ariga, J. A. Jackman, N.-J. Cho, S.-H. Hsu, L. K. Shrestha, T. Mori, J. Takeya, *Chem. Rec.* **2018,** *18*, 1.

[43] B. J. Finlayson-Pitts, J. N. Pitts, *Science* **1997,** *276*, 1045.

[44] J. L. C. Rowsell, E. C. Spencer, J. Eckert, J. A. K. Howard, O. M. Yaghi, *Science* **2005,** *309*, 1350.

[45] Y. Li, B. P. Bastakoti, M. Imura, J. Tang, A. Aldalbahi, N. L. Torad, Y. Yamauchi, *Chem. Eur. J.* **2015,** *21*, 6375.

[46] B. J. Melde, B. J. Johnson, *Anal. Bioanal. Chem.* **2010,** *398*, 1565.

[47] F. Hoffmann, M. Cornelius, J. Morell, M. Fröba, *Angew. Chem. Int. Ed.* **2006,** *45*, 3216.

[48] Y. Zhu, H. Li, Q. Zheng, J. Xu, X. Li, *Langmuir* **2012,** *28*, 7843.

[49] K. J. Lee, N. Shiratori, G. H. Lee, J. Miyawaki, I. Mochida, S. H. Yoon, J. Jang, *Carbon* **2010,** *48*, 4248.

[50] A. Palaniappan, X. Li, F. E. H. Tay, J. Li, X. Su, *Sensor. Actuat. B: Chem.* **2006,** *119*, 220.

[51] A. Palaniappan, X. Su, F. E. H. Tay, *J. Electroceram.* **2006,** *16*, 503.

[52] A. Palaniappan, X. Su, F. E. H. Tay, *IEEE Sensors Journal* **2006,** *6*, 1676.

[53] A. Palaniappan, S. Moochhala, F. E. H. Tay, N. C. L. Phua, X. Su, *Sensor. Actuat. B: Chem.* **2008,** *133*, 241.

[54] T. Lebold, L. A. Mühlstein, J. Blechinger, M. Riederer, H. Amenitsch, R. Köhn, K. Peneva, K. Müllen, J. Michaelis, C. Bräuchle, T. Bein, *Chem. Eur. J.* **2009,** *15*, 1661.

[55] F. Long, C. Gao, H. C. Shi, M. He, A. N. Zhu, A. M. Klibanov, A. Z. Gu, *Biosens. Bioelectron.* **2011,** *26*, 4018.

[56] Y. Tao, X. Li, T. Xu, H. Yu, P. Xu, B. Xiong, C. Wei, *Sensor. Actuat. B: Chem.* **2011,** *157*, 606.

[57] C. Guo, J. Irudayaraj, *Anal. Chem.* **2011,** *83*, 2883.

[58] T. Balaji, S. A. El-Safty, H. Matsunaga, T. Hanaoka, F. Mizukami, *Angew. Chem.* **2006,** *118*, 7360.

[59] D. Wen, L. Deng, S. Guo, S. Dong, *Anal. Chem.* **2011,** *83*, 3968.

[60] L. Mercier, T. J. Pinnavaia, *Environ. Sci. Technol.* **1998,** *32*, 2749.

[61] A. Bibby, L. Mercier, *Chem. Mater.* **2002,** *14*, 1591.

[62] E. Sumesh, M. S. Bootharaju, Anshup, T. Pradeep, *J. Hazard. Mater.* **2011,** *189*, 450.

[63] A. M. Liu, K. Hidajat, S. Kawi, D. Y. Zhao, *Chem. Commun.* **2000**, 1145.

[64] R. Métivier, I. Leray, B. Lebeau, B. Valeur, *J. Mater. Chem.* **2005,** *15*, 2965.

[65] H. Lou, Y. Zhang, Q. Xiang, J. Xu, H. Li, P. Xu, X. Li, *Sensor. Actuat. B: Chem.* **2012,** *166-167*, 246.

[66] N. L. Torad, H. Y. Lian, K. C. W. Wu, M. B. Zakaria, N. Suzuki, S. Ishihara, Q. Ji, M. Matsuura, K. Maekawa, K. Ariga, T. Kimura, Y. Yamauchi, *J. Mater. Chem.* **2012,** *22*, 20008.

[67] S. Higgins, W. DeSisto, D. Ruthven, *Micropor. Mesopor. Mater.* **2009,** *117*, 268.

[68] J. Crank, *The mathematics of diffusion, Clarendon Press, Oxford, 12nd Edn.* **1975**.

[69] H. K. Chagger, F. E. Ndaji, M. L. Sykes, K. M. Thomas, *Carbon* **1995,** *33*, 1405.

[70] Y. Zhu, H. Li, J. Xu, H. Yuan, J. Wang, X. Li, *CrystEngComm* **2011,** *13*, 402.

[71] S. K. Das, M. K. Bhunia, A. Bhaumik, *J. Solid State Chem.* **2010,** *183*, 1326.

[72] M. M. Ayad, N. A. Salahuddin, N. L. Torad, A. A. El-Nasr, *RSC Adv.* **2016,** *6*, 57929.

[73] C. Thörn, H. Gustafsson, L. Olsson, *Micropor. Mesopor. Mater.* **2013,** *176*, 71.

[74] H. Gustafsson, A. Küchler, K. Holmberg, P. Walde, *J. Mater. Chem. B* **2015,** *3*, 6174.

[75] G. Bayramoglu, V. C. Ozalp, M. Yilmaz, U. Guler, B. Salih, M. Y. Arica, *Micropor. Mesopor. Mater.* **2015,** *207*, 95.

[76] T. Kimura, N. L. Torad, Y. Yamauchi, *J. Mater. Chem. A* **2014,** *2*, 8196.

[77] J. Tang, N. L. Torad, R. R. Salunkhe, J.-H. Yoon, M. S. Al Hossain, S. X. Dou, J. H. Kim, T. Kimura, Y. Yamauchi, *Chem. Asian J.* **2014,** *9*, 3238.

[78] M. Brutschy, M. W. Schneider, M. Mastalerz, S. R. Waldvogel, *Adv. Mater.* **2012,** *24*, 6049.

[79] A. Y. Nazzal, L. Qu, X. Peng, M. Xiao, *Nano Lett.* **2003,** *3*, 819.

[80] Q. Kuang, C. Lao, Z. L. Wang, Z. Xie, L. Zheng, *J. Am. Chem. Soc.* **2007,** *129*, 6070.

[81] J. H. He, Y. Y. Zhang, J. Liu, D. Moore, G. Bao, Z. L. Wang, *J. Phys. Chem. C* **2007,** *111*, 12152.

[82] M. J. S. Spencer, *Prog. Mater. Sci.* **2012,** *57*, 437.

[83] M. Müllner, T. Lunkenbein, M. Schieder, A. H. Gröschel, N. Miyajima, M. Förtsch, J. Breu, F. Caruso, A. H. E. Müller, *Macromolecules* **2012,** *45*, 6981.

[84] N. Yamazoe, Y. Kurokawa, T. Seiyama, *Sensor. Actuat.* **1983,** *4*, 283.

[85] A. Yu, Z. Liang, J. Cho, F. Caruso, *Nano Lett.* **2003,** *3*, 1203.

[86] Y. Zhang, Z. Zheng, F. Yang, *Ind. Eng. Chem. Res.* **2010,** *49*, 3539.

[87] E. Redel, E. Arsenault, P. G. O'Brien, N. P. Kherani, G. A. Ozin, *Chem. Mater.* **2011,** *23*, 1353.

[88] N. G. Cho, H. S. Woo, J. H. Lee, I. D. Kim, *Chem. Commun.* **2011,** *47*, 11300.

[89] G. Xi, J. Ye, Q. Ma, N. Su, H. Bai, C. Wang, *J. Am. Chem. Soc.* **2012,** *134*, 6508.

[90] C. Wang, R. L. Thompson, J. Baltrus, C. Matranga, *J. Phys. Chem. Lett.* **2010,** *1*, 48.

[91] L. Francioso, D. S. Presicce, P. Siciliano, A. Ficarella, *Sensor. Actuat. B: Chem.* **2007,** *123*, 516.

[92] A. Galińska, J. Walendziewski, *Energ. Fuel.* **2005,** *19*, 1143.

[93] E. G. Karpov, M. A. Hashemian, S. K. Dasari, *J. Phys. Chem. C* **2013,** *117*, 15632.

[94] S. Y. Huang, P. Ganesan, S. Park, B. N. Popov, *J. Am. Chem. Soc.* **2009,** *131*, 13898.

[95] H. A. Harms, N. Tétreault, V. Gusak, B. Kasemo, M. Grätzel, *Phys. Chem. Chem. Phys.* **2012,** *14*, 9037.

[96] B. P. Bastakoti, N. L. Torad, Y. Yamauchi, *ACS Appl. Mater. Interfaces* **2014,** *6*, 854.

[97] *IARC Monographs on the Evaluation of Carcinogenic Risks to Humans, WHO-IARC: Lyon, France, 1999, 71*, 14.

[98] M. Zhang, Z. Yuan, J. Song, C. Zheng, *Sensor. Actuat. B: Chem.* **2010,** *148*, 87.

[99] L. Francioso, D. S. Presicce, P. Siciliano, A. Ficarella, *Sensors and Actuators B: Chemical* **2007,** *123*, 516.

[100] M. Epifani, T. Andreu, R. Zamani, J. Arbiol, E. Comini, P. Siciliano, G. Faglia, J. R. Morante, *CrystEngComm* **2012,** *14*, 3882.

[101] J. L. Falconer, K. A. Magrini-Bair, *J. Catal.* **1998,** *179*, 171.

[102] M. A. Ponce, R. Parra, R. Savu, E. Joanni, P. R. Bueno, M. Cilense, J. A. Varela, M. S. Castro, *Sensor. Actuat. B: Chem.* **2009,** *139*, 447.

[103] F. Razzaghi, C. Debiemme-Chouvy, F. Pillier, H. Perrot, O. Sel, *Phys. Chem. Chem. Phys.* **2015,** *17*, 14773.

[104] B. Liu, Q. Li, B. Zhang, Y. Cui, H. Chen, G. Chen, D. Tang, *Nanoscale* **2011,** *3*, 2220.

[105] J. W. Lee, S. H. Nam, J. H. Yu, D. I. Kim, R. H. Jeong, J. H. Boo, *Applied Surface Science* **2018**.

[106] N. Horzum, D. Tascioglu, C. Özbek, S. Okur, M. M. Demir, *New J. Chem.* **2014,** *38*, 5761.

[107] S. Baek, W. Kim, S. Jeon, K. Yong, *Sensor. Actuat. B: Chem.* **2018,** *262*, 595.

[108] J. Tang, J. Liu, R. R. Salunkhe, T. Wang, Y. Yamauchi, *Chem. Commun.* **2016,** *52*, 505.

[109] K. Ariga, A. Vinu, Q. Ji, O. Ohmori, J. P. Hill, S. Acharya, J. Koike, S. Shiratori, *Angew. Chem. Int. Ed.* **2008,** *47*, 7254.

[110] Q. Ji, S. B. Yoon, J. P. Hill, A. Vinu, J. S. Yu, K. Ariga, *J. Am. Chem. Soc.* **2009,** *131*, 4220.

[111] L. Jia, G. P. Mane, C. Anand, D. S. Dhawale, Q. Ji, K. Ariga, A. Vinu, *Chem. Commun.* **2012,** *48*, 9029.

[112] L. Jia, H. Wang, D. Dhawale, C. Anand, M. A. Wahab, Q. Ji, K. Ariga, A. Vinu, *Chem. Commun.* **2014,** *50*, 5976.

[113] Y. Kosaki, H. Izawa, S. Ishihara, K. Kawakami, M. Sumita, Y. Tateyama, Q. Ji, V. Krishnan, S. Hishita, Y. Yamauchi, J. P. Hill, A. Vinu, S. Shiratori, K. Ariga, *ACS Appl. Mater. Interfaces* **2013,** *5*, 2930.

[114] G. P. Mane, S. N. Talapaneni, C. Anand, S. Varghese, H. Iwai, Q. Ji, K. Ariga, T. Mori, A. Vinu, *Adv. Funct. Mater.* **2012,** *22*, 3596.

[115] G. P. Mane, D. S. Dhawale, C. Anand, K. Ariga, Q. Ji, M. A. Wahab, T. Mori, A. Vinu, *J. Mater. Chem. A* **2013,** *1*, 2913.

[116] E. S. Mañoso, R. Herrera-Basurto, B. M. Simonet, M. Valcárcel, *Sensor. Actuat. B Chem.* **2013,** *186*, 811.

[117] A. L. Ndiaye, J. Brunet, C. Varenne, A. Pauly, *J. Phys. Chem. C* **2018,** *122*, 21632.

[118] C. Yu Shiun, H. Yao Ching, C. Jin Chern, W. Hui Liang, H. Hung Shu, H. Li Chia, H. Guewha Steven, *Jpn. J. Appl. Phys.* **2010,** *49*, 105103.

[119] J. Wu, W. Pisula, K. Müllen, *Chem. Rev.* **2007,** *107*, 718.

[120] E. Yoo, J. Kim, E. Hosono, H. S. Zhou, T. Kudo, I. Honma, *Nano Lett.* **2008,** *8*, 2277.

[121] C. H. Lu, H. H. Yang, C. L. Zhu, X. Chen, G. N. Chen, *Angew. Chem.* **2009,** *121*, 4879.

[122] Z. Cheng, Q. Li, Z. Li, Q. Zhou, Y. Fang, *Nano lett.* **2010,** *10*, 1864.

[123] Y. Song, K. Qu, C. Zhao, J. Ren, X. Qu, *Adv. Mater.* **2010,** *22*, 2206.

[124] Q. Ji, I. Honma, S. M. Paek, M. Akada, J. P. Hill, A. Vinu, K. Ariga, *Angew. Chem. Int. Ed.* **2010,** *49*, 9737.

[125] H. Jin, X. Tao, B. Feng, L. Yu, D. Wang, S. Dong, J. Luo, *Vacuum* **2017,** *140*, 101.

[126] S. Wang, G. Xie, Y. Su, L. Su, Q. Zhang, H. Du, H. Tai, Y. Jiang, *Sensor. Actuat. B Chem.* **2018,** *255*, 2203.

[127] X. Deng, M. Chen, Q. Fu, N. M. B. Smeets, F. Xu, Z. Zhang, C. D. M. Filipe, T. Hoare, *ACS Appl. Mater. Interfaces* **2016,** *8*, 1893.

[128] C. Dey, T. Kundu, B. P. Biswal, A. Mallick, R. Banerjee, *Acta Crystallogr. B* **2014,** *70*, 3.

[129] C. Y. Huang, M. Song, Z. Y. Gu, H. F. Wang, X. P. Yan, *Environ. Sci. Technol.* **2011,** *45*, 4490.

[130] M. Meilikhov, S. Furukawa, K. Hirai, R. A. Fischer, S. Kitagawa, *Angew. Chem. Int. Ed.* **2012,** *125*, 359.

[131] M. Tu, S. Wannapaiboon, K. Khaletskaya, R. A. Fischer, *Adv. Funct. Mater.* **2015,** *25*, 4470.

[132] A. Bétard, R. A. Fischer, *Chem. Rev.* **2012,** *112*, 1055.

[133] O. Shekhah, H. Wang, S. Kowarik, F. Schreiber, M. Paulus, M. Tolan, C. Sternemann, F. Evers, D. Zacher, R. A. Fischer, C. Wöll, *J. Am. Chem. Soc.* **2007,** *129*, 15118.

[134] O. Shekhah, H. Wang, D. Zacher, R. A. Fischer, C. Wöll, *Angew. Chem. Int. Ed.* **2009,** *48*, 5038.

[135] A. Bétard, S. Wannapaiboon, R. A. Fischer, *Chem. Commun.* **2012,** *48*, 10493.

[136] L. Heinke, Z. Gu, C. Wöll, *Nat. commun.* **2014,** *5*, 4562.

[137] S. Achmann, G. Hagen, J. Kita, I. M. Malkowsky, C. Kiener, R. Moos, *Sensors* **2009,** *9*, 1574.

[138] J. Devkota, K.-J. Kim, P. R. Ohodnicki, J. T. Culp, D. W. Greve, J. W. Lekse, *Nanoscale* **2018,** *10*, 8075.

[139] M. D. Allendorf, R. J. Houk, L. Andruszkiewicz, A. A. Talin, J. Pikarsky, A. Choudhury, K. A. Gall, P. J. Hesketh, *J. Am. Chem. Soc.* **2008,** *130*, 14404.

[140] I. Ellern, A. Venkatasubramanian, J. H. Lee, P. J. Hesketh, V. Stavilla, M. D. Allendorf, A. L. Robinson, *ECS Transactions* **2013,** *50*, 469.

[141] L. Kosuru, A. Bouchaala, N. Jaber, M. I. Younis, *Journal of Sensors* **2016,** *2016*.

[142] A. Venkatasubramanian, M. Navaei, K. R. Bagnall, K. C. McCarley, S. Nair, P. J. Hesketh, *J. Phys. Chem. C* **2012,** *116*, 15313.

[143] H. Yamagiwa, S. Sato, T. Fukawa, T. Ikehara, R. Maeda, T. Mihara, M. Kimura, *Sci. Rep.* **2014,** *4*, 6247.

[144] K. Ariga, Y. Yamauchi, T. Mori, J. P. Hill, *Adv. Mater.* **2013,** *25*, 6477.

[145] M. Tsotsalas, A. Umemura, F. Kim, Y. Sakata, J. Reboul, S. Kitagawa, S. Furukawa, *J. Mater. Chem.* **2012,** *22*, 10159.

[146] J. Benito, M. Fenero, S. Sorribas, B. Zornoza, K. J. Msayib, N. B. McKeown, C. Téllez, J. Coronas, I. Gascón, *Colloids Surf. A* **2015,** *470*, 161.

[147] J. Benito, S. Sorribas, I. Lucas, J. Coronas, I. Gascon, *ACS Appl. Mater. Interfaces* **2016,** *8*, 16486.

[148] X. Fang, L. Wang, X. He, J. Xu, Z. Duan, *Inorg. Chem.* **2018,** *57*, 1689.

[149] M. A. Andrés, M. Benzaqui, C. Serre, N. Steunou, I. Gascón, *J. Colloid Interface Sci.* **2018,** *519*, 88.

[150] F. Xu, L. Sun, P. Huang, Y. Sun, Q. Zheng, Y. Zou, H. Chu, E. Yan, H. Zhang, J. Wang, Y. Du, *Sensor. Actuat. B Chem.* **2018,** *254*, 872.

[151] M. Hu, S. Furukawa, R. Ohtani, H. Sukegawa, Y. Nemoto, J. Reboul, S. Kitagawa, Y. Yamauchi, *Angew. Chem. Int. Ed.* **2012,** *51*, 984.

[152] P. A. Berseth, J. J. Sokol, M. P. Shores, J. L. Heinrich, J. R. Long, *J. Am. Chem. Soc.* **2000,** *122*, 9655.

[153] K. Nakatani, P. Yu, *Adv. Mater.* **2001,** *13*, 1411.

[154] P. Zhou, D. Xue, H. Luo, X. Chen, *Nano Lett.* **2002,** *2*, 845.

[155] M. Pyrasch, A. Toutianoush, W. Jin, J. Schnepf, B. Tieke, *Chem. Mater.* **2003,** *15*, 245.

[156] T. Uemura, S. Kitagawa, *J. Am. Chem. Soc.* **2003,** *125*, 7814.

[157] T. Uemura, M. Ohba, S. Kitagawa, *Inorg. Chem.* **2004,** *43*, 7339.

[158] R. Chen, M. Asai, C. Fukushima, M. Ishizaki, M. Kurihara, M. Arisaka, T. Nankawa, M. Watanabe, T. Kawamoto, H. Tanaka, *J. Radioanal. Nucl. Chem.* **2015,** *303*, 1491.

[159] R. Chen, H. Tanaka, T. Kawamoto, M. Asai, C. Fukushima, H. Na, M. Kurihara, M. Watanabe, M. Arisaka, T. Nankawa, *Electrochim. Acta* **2013,** *87*, 119.

[160] R. Chen, H. Tanaka, T. Kawamoto, M. Asai, C. Fukushima, M. Kurihara, M. Ishizaki, M. Watanabe, M. Arisaka, T. Nankawa, *ACS Applied Materials & Interfaces* **2013,** *5*, 12984.

[161] N. L. Torad, M. Hu, M. Imura, M. Naito, Y. Yamauchi, *J. Mater. Chem.* **2012,** *22*, 18261.

[162] M. Hu, N. L. Torad, Y. D. Chiang, K. C. W. Wu, Y. Yamauchi, *CrystEngComm* **2012,** *14*, 3387.

[163] M. Hu, N. L. Torad, Y. Yamauchi, *Eur. J. Inorg. Chem.* **2012,** *2012*, 4795.

[164] Y. Kamachi, M. B. Zakaria, N. L. Torad, T. Nakato, T. Ahamad, S. M. Alshehri, V. Malgras, Y. Yamauchi, *J. Nanosci. Nanotechnol.* **2016,** *16*, 4200.

[165] T. Lee, Z. X. Liu, H. L. Lee, *Cryst. Growth Des.* **2011,** *11*, 4146.

[166] P. Á. Szilágyi, R. J. Westerwaal, R. van de Krol, H. Geerlings, B. Dam, *J. Mater. Chem. C* **2013,** *1*, 8146.

[167] D. J. Wales, J. Grand, V. P. Ting, R. D. Burke, K. J. Edler, C. R. Bowen, S. Mintova, A. D. Burrows, *Chem. Soc. Rev.* **2015,** *44*, 4290.

[168] N. Bakhtiari, S. Azizian, S. M. Alshehri, N. L. Torad, V. Malgras, Y. Yamauchi, *Micropor. Mesopor. Mater.* **2015,** *217*, 173.

[169] N. L. Torad, M. Hu, S. Ishihara, H. Sukegawa, A. A. Belik, M. Imura, K. Ariga, Y. Sakka, Y. Yamauchi, *Small* **2014,** *10*, 2096.

[170] A. Comotti, S. Bracco, P. Sozzani, S. Horike, R. Matsuda, J. Chen, M. Takata, Y. Kubota, S. Kitagawa, *J. Am. Chem. Soc.* **2008,** *130*, 13664.

[171] N. L. Torad, M. Hu, Y. Kamachi, K. Takai, M. Imura, M. Naito, Y. Yamauchi, *Chem. Commun.* **2013,** *49*, 2521.

[172] M. Hu, J. Reboul, S. Furukawa, N. L. Torad, Q. Ji, P. Srinivasu, K. Ariga, S. Kitagawa, Y. Yamauchi, *J. Am. Chem. Soc.* **2012,** *134*, 2864.

[173] M. P. Pina, R. Mallada, M. Arruebo, M. Urbiztondo, N. Navascués, O. de la Iglesia, J. Santamaria, *Micropor. Mesopor. Mater.* **2011,** *144*, 19.

[174] Y. Yan, T. Bein, *Chem. Mater.* **1992,** *4*, 975.

[175] S. Mintova, T. Bein, *Micropor. Mesopor. Mater.* **2001,** *50*, 159.

[176] S. Mintova, S. Mo, T. Bein, *Chem. Mater.* **2001,** *13*, 901.

[177] M. Osada, I. Sasaki, M. Nishioka, M. Sadakata, T. Okubo, *Micropor. Mesopor. Mater.* **1998,** *23*, 287.

[178] I. Sasaki, H. Tsuchiya, M. Nishioka, M. Sadakata, T. Okubo, *Sensor. Actuat. B: Chem.* **2002,** *86*, 26.

[179] H. Huang, J. Zhou, S. Chen, L. Zeng, Y. Huang, *Sensor. Actuat. B: Chem.* **2004,** *101*, 316.

[180] E. Biemmi, T. Bein, *Langmuir* **2008,** *24*, 11196.

[181] X. Ji, W. Yao, J. Peng, N. Ren, J. Zhou, Y. Huang, *Sensor. Actuat. B: Chem.* **2012,** *166-167*, 50.

[182] N. L. Torad, M. Naito, J. Tatami, A. Endo, S. Y. Leo, S. Ishihara, K. C. W. Wu, T. Wakihara, Y. Yamauchi, *Chem. Asian J.* **2014,** *9*, 759.